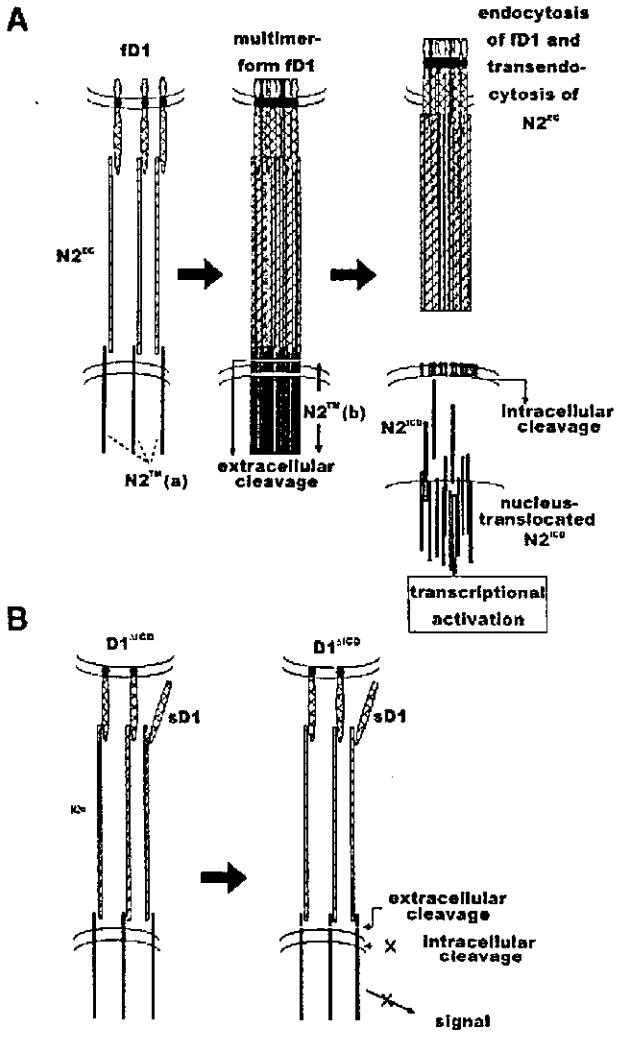

Fig. 7. Scheme of the ligand-induced cleavage of Notch receptor. (A) Upon binding to the Notch receptor, fNL forms appropriate homomultimers, leading to the intracellular cleavage of Notch in addition to the extracellular cleavage. Cleaved N^{ICD} translocates into the nucleus. Endocytosis of NL and N^{EC} occurs at some time point during the series of process. (B) $NL\Delta^{ICD}$ or sNL can bind to the Notch receptor and cleave Notch at the extracellular site, but do not form appropriate multimers or excute the intracellular cleavage of Notch, resulting in the failure of the Notch activation.

dominant-negative activity of $D1\Delta^{ICD}$ was likely to occur via interaction with fD1 rather than simple binding competition, raising the possibility that NL molecules interact with each other. Therefore, we investigated whether the signal-transducing activity of sD1–Fc was enhanced by addition of an anti-Fc polyclonal antibody, which can cross-link the sD1–Fc molecules. Results showed that addition of the anti-Fc antibody significantly increased the signal-transducing activity of sD1–Fc, but not of control IgG, in a dose-dependent manner (Figure 6C). We also note that the same phenomenon also occurred using soluble Jagged1 protein fused to Fc (data not shown). These results suggest that multimerization of the Notch ligand plays an important role in full activation of N2 (see Figure 7).

Discussion

In this study, we compared the signal-transducing activity of sD1 and fD1 and used the resultant information to analyze the activation process of N2 after ligand stimulation. We found that sD1 functions as a partial agonist and that the mechanism of such a function could stem from the incomplete activity of sD1 in the intracellular cleavage required to release $N2^{ICD}$. Furthermore, experiments using sD1 and $D1\Delta^{ICD}$ demonstrated that the extracellular cleavage at the extracellular domain of N2 does not autonomously induce intracellular cleavage, which takes place in the transmembrane domain, and that $D1^{ICD}$ is involved in some unidentified mechanisms that exist between the two cleavage processes. Given that the signal-transducing activity of sD1–Fc was enhanced by the addition of an anti-Fc antibody and that $D1\Delta^{ICD}$ acted in a dominant-negative fashion against fD1 for N2 signaling, we suggest that multimerization of NL would be important for intracellular cleavage (Figure 7).

A soluble form of *Drosophila* Delta does exist *in vivo* (Klueg *et al.*, 1998), possibly generated by Kuzbanian (Qi *et al.*, 1999). Therefore, it is important to understand the exact physiological function of sNL, although the precise C-terminal sequence of naturally occurring soluble Delta is unknown. However, conclusions regarding the biological activity of sNL to date have been discordant, as manoeuvered mammalian sD1 and soluble Jagged1 have been characterized as having an agonistic activity in *in vitro* experiments (Li *et al.*, 1998; Qi *et al.*, 1999; Han *et al.*, 2000; Karanu *et al.*, 2000; Morrison *et al.*, 2000) and an antagonistic activity has been proposed for soluble Delta and Serrate in *Drosophila in vivo* assessments (Hukriede *et al.*, 1997; Sun and Artavanis-Tsakonas, 1997). Examination of this issue was enabled by transcriptional activation assay using CHO(r) cells over-expressing mouse fN2 (fN2-CHO) (Shimizu *et al.*, 2000), which is a very sensitive system. We have demonstrated that sD1 comprising entire extracellular domain induces N2 activation, but the activity is markedly lower than that induced by fD1 (Figure 1A). This indicates that sD1 is a partial agonist, while fD1 is a full activator for Notch signaling. The fact that the coexistence of sD1 led to inhibition of fD1-induced N2 activation (Figure 1C) further supports the nature of sD1 as a partial agonist. We also note that the signal-transducing activity of soluble Jagged1-Fc is lower than that of full-length Jagged1 (data not shown). Hence, a partial activity in the soluble form may be common to all kinds of NL, including naturally existing sNL, since they do not harbor NL^{ICD} that is essential for full activation of Notch signaling (Figure 5); this scenario explains the contradiction concerning the biological activity of sNL. Regarding the physiological function of sNL *in vivo*, we speculate that it is associated with the strict control of the Notch signaling, which is known to be critical for the exact cell fate decision, because the abnormal phenotype is seen in patients with haploinsufficiency of Jagged1 (Li *et al.*, 1997; Oda *et al.*, 1997).

In an analysis tracing the N2 fragments, we ascertained the molecular basis of the incomplete function of sD1. Consistent with the low transcriptional activity of sD1 (Figure 1A), the stimulation with sD1–Fc did not result in

nuclear accumulation of $N2^{ICD}$ (Figure 2), whose amount is considered to determine the level of subsequent RBP-Jκ-mediated transcriptional activation (Jarriault *et al.*, 1995; Schroeter *et al.*, 1998). Furthermore, the experiments using sD1–Fc incidentally unveiled the mechanism of the cleavage of $N2^{TM}$ in the extracellular region (Figures 2 and 3), which was recently demonstrated by different approaches (Brou *et al.*, 2000; Mumm *et al.*, 2000). This cleavage was also evident after the binding of fD1 (Figure 4), but only when the intracellular cleavage that takes place in the transmembrane portion of $N2^{TM}$ was blocked by an inhibitor (Figure 4D). Taken together, these data imply that sD1 induces the extracellular cleavage of N2, but fails to sufficiently promote the intracellular cleavage that releases $N2^{ICD}$, while fD1 efficiently triggers both cleavages. This indicates that the extracellular domain of Notch ligand alone is sufficient for extracellular cleavage of N2, and that extracellular cleavage is not necessarily followed by progression to intracellular cleavage, suggesting the existence of an as yet unknown mechanism regulating activation of the intracellular cleavage.

However, this notion was controversial, being in contrast to the recent report on extracellular cleavage of N1 in which the intracellular cleavage and subsequent signal transduction are described as autonomous events after extracellular cleavage (Mumm *et al.*, 2000), which was drawn from experiments using the truncated N1 protein lacking N^{EC}. Regarding this discrepancy, we raise the possibility that the intracellular cleavage in the truncated Notch protein lacking N^{EC} progresses through a mechanism different from the intracellular cleavage induced by a ligand in the natural Notch protein. Indeed, the difference in intracellular cleavage between the two molecules was reported; the intracellular cleavage in the natural Notch protein occurred within 15 min of ligand binding (Shimizu *et al.*, 2000), whereas that in the truncated Notch protein required >60 min (Schroeter *et al.*, 1998) after protein synthesis. In addition, we also found that the amino acid sequence surrounding the extracellular cleavage site identified using truncated N1 (Brou *et al.*, 2000; Mumm *et al.*, 2000) is not conserved in N2. Consistent with this, addition of 1,10-*o*-phenanthroline, a reagent identified as an inhibitor of the extracellular cleavage in truncated Notch1 (Mumm *et al.*, 2000), did not prevent sD1–Fc-induced extracellular cleavage of N2 (data not shown). Therefore, the extracellular cleavage site and the activation mechanism required for intracellular cleavage in the mutant Notch protein lacking N^{EC} may be somewhat diverse from those in the natural Notch proteins. Alternatively, the discrepancy may result from an unidentified difference between N1 and N2.

One clue to the mechanism regulating activation of the intracellular cleavage was found in the data from experiments using the truncated Dl protein lacking its ICD, $D1\Delta^{ICD}$ (Figure 5). The characteristics of $D1\Delta^{ICD}$ are similar to those of sD1 rather than those of fD1, i.e. a low level of transcriptional activity from the TP-1 promoter, sufficiency in cleaving the extracellular domain of $N2^{TM}$, and insufficiency in cleaving $N2^{TM}$ within the transmembrane portion and in releasing $N2^{ICD}$, although there was a slight difference in the emergence of $N2^{TM}$(b) (Figure 5B and C). These indicate that ICD of Delta1 is indispensable for the cleavage of $N2^{TM}$ within its transmembrane portion, which is essential for full activation of N2 (Figure 7).

Another clue to the mechanism lies in the data from experiments using sD1–Fc plus an anti-Fc antibody. Addition of the anti-Fc antibody resulted in enhancement of the signal-transducing activity of sD1–Fc (Figure 6C), suggesting that multimerization of the ligand is associated with the full activation of N2 (Figure 7). Dimerization of NL is inefficient, since the signal-transducing activities of sD1–Fc (dimer) and sD1-Flag(His_6) (monomer) were the same (Figure 1). It is possible that an assembly of a large number of NL molecules is required for fN activation, since a monoclonal anti-Fc antibody did not work, unlike a polyclonal antibody (data not shown). Putting together the inevitable role of $D1^{ICD}$ for D1-induced N2 intracellular cleavage and subsequent N2 activation, as we discussed above, NL^{ICD} may be the region that is used for the multimerization of fNL. As for the strong dominant-negative effect of $D1\Delta^{ICD}$ against fD1 (Figure 6), we raise the possibility that $D1\Delta^{ICD}$ can interact with fD1 using its transmembrane and/or extracellular domains to participate in the fD1 assembly, which interfere with the appropriate fD1 multimerization suitable for the intracellular cleavage of N2.

As is well known with regard to cytokines and their receptor systems (reviewed in Heldin, 1995), the multimerization of NL may be associated with the assembly of the Notch receptor, which may result in its conformational change and allow the transmembrane domain of Notch to be subjected to the action of the presenilin-containing protease complex and subsequent cleavage. Upon fD1 binding, N2 extracellular cleavage must be preceeded by fD1 multimerization and N2 assembly, although these steps are not necessary for N2 extracellular cleavage itself (Figure 7).

It was reported recently that transendocytosis by the ligand-expressing cells of the ligand-bound Notch extracellular domain together with the ligand appears to be necessary for efficient Notch processing and signal transduction (Parks *et al.*, 2000). Integrating this into our model of Notch receptor activation, the endocytosis process may be positioned after the ligand multimerization or Notch assembly. However, we are not certain whether the transendocytosis is always necessary for the Notch signaling, since cell-free ligands can activate Notch signaling, particularly when the antibody-mediated ligand cross-linking or ligand-coating technique is used (Figure 6; Morrison *et al.*, 2000; Varnum-Finney *et al.*, 2000). Given the well-established notion in the G-coupled receptor and the cytokine receptor systems that endocytosis is associated with receptor/ligand degradation rather than directly associated with signal activation, the possibility may remain that transendocytosis in the Notch signaling pathway participates in degradation of Notch and NL.

Comparing the effect of $D1\Delta^{ICD}$ with that of sD1, emergence of $N2^{TM}$(b) was less clear when stimulated with the former (Figures 2 and 3) than that with the latter (Figure 5C), despite our assumption that $N2^{TM}$(b) was indeed generated after $D1\Delta^{ICD}$ stimulation, since the amount of $N2^{TM}$(a) was obviously reduced. As an explanation of this phenomenon, we speculate that some

unknown degradation process for $N2^{TM}$(b) is accelerated by stimulation with $D1\Delta^{ICD}$ but not with sD1.

In the present study, we demonstrated the biological activities of sNL and the existence of a novel mechanism involved in the activation of the Notch receptor by its ligand. Although many investigators are using sNL to determine the involvement of the Notch signal in the regulation of cell differentiation in various experimental approaches, we have to be careful of the interpretation of results, since the demonstrated phenotype could be caused by the inhibition, rather than activation, of the Notch signal. We believe that the findings described here will facilitate understanding of the complexities of Notch signaling in higher vertebrates.

Materials and methods

Plasmid construction

To generate $D1\Delta^{ICD}$, mouse *Delta1* cDNA (a gift from A.Gossler; Bettenhausen *et al.*, 1995) was truncated at the codon CGG corresponding to arginine (amino acid 570). The resulting $D1^{DICD}$ was constructed in an expression vector pTraserCMV (Clontech) after addition of a Flag or a Myc tag.

Soluble fusion proteins

sD1 proteins [sD1–Fc and sD1-Flag$(His)_6$] and sN1 protein (sN1-Fc) were prepared as described previously (Shimizu *et al.*, 1999, 2000).

Cell culture

BaF3 cells were maintained in RPMI medium supplemented with 10% fetal bovine serum (FBS) and 0.5 ng/ml recombinant mouse interleukin-3 (a gift from Kirin Brewery, Japan). CHO(r) (a gift from S.Shirahata, Kyushu University), fN2-CHO (Shimizu *et al.*, 2000), fD1-CHO (Shimizu *et al.*, 2000), $D1\Delta^{ICD}$-CHO and fD1/$D1\Delta^{ICD}$-CHO cells were maintained in alpha-minimal essential medium containing 10% FBS.

Antibody

An anti-human IgG goat polyclonal antibody used for multimerization of sD1–Fc was purchased from DAKO Japan Co., Ltd.

Cell-binding assay

Binding of sD1–Fc to the pro-B cell line BaF3 was performed as described previously (Shimizu *et al.*, 1999), with the minor modification that the binding reaction was terminated at 5 min.

Co-precipitation using sD1–Fc

Co-precipitation using sD1–Fc has been described elsewhere (Shimizu *et al.*, 2000). Disuccinimidyl glutarate (Pierce) was used to cross-link sD1–Fc and the bound Notch receptor.

Cell–cell association assay

Cell–cell association assay was performed as described previously (Shimizu *et al.*, 2000). Briefly, CHO(r) and fD1-CHO cells were inoculated at 1×10^6 into a 6 cm plate. After overnight culture, 1×10^6 BaF3 cells were spread over the monolayer of cells. Following co-culture at 37°C for the time indicated in Figure 4C, BaF3 cells that did not adhere to the cell layer were collected by swirling the plate very gently and washing the wells gently once with RPMI medium. The population obtained through these procedures was defined as non-adhered BaF3. Next, phosphate-buffered saline containing 2 mM EGTA was added to the wells and the BaF3 cells adhering to the cell layer were allowed to dissociate by tapping the plate. These BaF3 cells, together with additional cells collected by washing with RPMI medium, were defined as adhered BaF3. The cells in each fraction were then counted.

Transient transcription assay

A total of 4×10^4 fN2-CHO was inoculated into a 24-well plate and transfected with a TP1-luciferase reporter plasmid (Minoguchi *et al.*, 1997), pGa981-6, by a liposome-based method (SuperFect, Qiagen). Following transfection, sD1–Fc and sD1-Flag$(His)_6$ were added at the respective concentrations shown in Figure 1A and cultured for 30–40 h. When fD1 or $D1\Delta^{ICD}$ were used as a stimulator, these cells were added at 5×10^4 to the pGa981-6-transfected fN2-CHO and co-cultured for 30–40 h. The mixture of cells was then used for luciferase assay.

Subcellular fractionation of BaF3

After 1.5 h co-culture with fD1-CHO or $D1\Delta^{ICD}$-CHO, BaF3 was collected and membrane/cytosol-rich and nucleus-rich fractions were prepared as described elsewhere (Shimizu *et al.*, 2000). The membrane/cytosol-rich fraction was further centrifuged at 105 000 *g* for 30 min at 4°C to separate the membrane (pellet) and the cytosol (supernatant) fractions. These fractions were used for immunoprecipitation with an anti-N2 polyclonal antibody.

Acknowledgements

We thank Dr S.Artavanis-Tsakonas for providing us with the bhN6 anti-N2 antibody, Dr A.Gossler for mouse Delta1 cDNA, Dr T.Honjo for pGa981-6 plasmid and Dr S.Shirahata for CHO ras clone-I cells. We also wish to thank Mr Chris W.P.Reynolds for his review of the manuscript. This work was supported by grants-in-aid from the Ministry of Education, Science, Sport, Culture and Technology of Japan, and the Ministry of Health, Welfare and Labor of Japan.

References

Artavanis-Tsakonas,S., Rand,M.D. and Lake,R.J. (1999) Notch signaling: cell fate control and signal integration in development. *Science*, **284**, 770–776.

Bettenhausen,B., Hrabe de Angelis,M., Simon,D., Guenet,J. and Gossler,A. (1995) Transient and restricted expression during mouse embryogenesis of Dll1, a murine gene closely related to *Drosophila* Delta. *Development*, **121**, 2407–2418.

Blaumueller,C.M., Qi,H., Zagouras,P. and Artavanis-Tsakonas,S. (1997) Intracellular cleavage of Notch leads to a heterodimeric receptor on the plasma membrane. *Cell*, **90**, 281–291.

Brou,C. *et al.* (2000) A novel proteolytic cleavage involved in Notch signaling: the role of the disintegrin-metalloprotease TACE. *Mol. Cell*, **5**, 207–216.

Chan,Y.M. and Jan,Y.N. (1998) Roles for proteolysis and trafficking in notch maturation and signal transduction. *Cell*, **94**, 423–426.

Chitnis,A., Henrique,D., Lewis,J., Ish-Horowicz,D. and Kintner,C. (1995) Primary neurogenesis in *Xenopus* embryos regulated by a homologue of the *Drosophila* neurogenic gene Delta. *Nature*, **375**, 761–766.

De Strooper,B. *et al.* (1999) A presenilin-1-dependent gamma-secretase-like protease mediates release of Notch intracellular domain. *Nature*, **398**, 518–522.

Ellisen,L.W., Bird,J., West,D.C., Soreng,A.L., Reynolds,T.C., Smith,S.D. and Sklar,J. (1991) TAN-1, the human homolog of the *Drosophila* notch gene, is broken by chromosomal translocations in T lymphoblastic neoplasms. *Cell*, **66**, 649–661.

Greenwald,I. (1998) LIN-12/Notch signaling: lessons from worms and flies. *Genes Dev.*, **12**, 1751–1762.

Han,W., Ye,Q. and Moore,M.A. (2000) A soluble form of human Delta-like-1 inhibits differentiation of hematopoietic progenitor cells. *Blood*, **95**, 1616–1625.

Heldin,C.H. (1995) Dimerization of cell surface receptors in signal transduction. *Cell*, **80**, 213–223.

Hukriede,N.A., Gu,Y. and Fleming,R.J. (1997) A dominant-negative form of Serrate acts as a general antagonist of Notch activation. *Development*, **124**, 3427–3437.

Jarriault,S., Brou,C., Logeat,F., Schroeter,E.H., Kopan,R. and Israel,A. (1995) Signalling downstream of activated mammalian Notch. *Nature*, **377**, 355–358.

Jarriault,S., Le Bail,O., Hirsinger,E., Pourquie,O., Logeat,F., Strong,C.F., Brou,C., Seidah,N.G. and Israel,A. (1998) Delta-1 activation of notch-1 signaling results in HES-1 transactivation. *Mol. Cell. Biol.*, **18**, 7423–7431.

Jen,W.C., Wettstein,D., Turner,D., Chitnis,A. and Kintner,C. (1997) The Notch ligand, X-Delta-2, mediates segmentation of the paraxial mesoderm in *Xenopus* embryos. *Development*, **124**, 1169–1178.

Karanu,F.N., Murdoch,B., Gallacher,L., Wu,D.M., Koremoto,M., Sakano,S. and Bhatia,M. (2000) The notch ligand jagged-1 represents a novel growth factor of human hematopoietic stem cells. *J. Exp. Med.*, **192**, 1365–1372.

Klueg,K.M., Parody,T.R. and Muskavitch,M.A. (1998) Complex

proteolytic processing acts on Delta, a transmembrane ligand for Notch, during *Drosophila* development. *Mol. Biol. Cell*, **9**, 1709–1723.

Kopan,R. and Weintraub,H. (1993) Mouse notch: expression in hair follicles correlates with cell fate determination. *J. Cell Biol.*, **3**, 631–641.

Kopan,R., Schroeter,E.H., Weintraub,H. and Nye,J.S. (1996) Signal transduction by activated mNotch: importance of proteolytic processing and its regulation by the extracellular domain. *Proc. Natl Acad. Sci. USA*, **93**, 1683–1688.

Lardelli,M., Dahlstrand,J. and Lendahl,U. (1994) The novel Notch homologue mouse Notch3 lacks specific epidermal growth factor repeats and is expressed in proliferating neuroepithelium. *Mech. Dev.*, **46**, 123–136.

Li,L. *et al.* (1997) Alagille syndrome is caused by mutations in human Jagged1, which encodes a ligand for Notch1. *Nature Genet.*, **16**, 243–251.

Li,L. *et al.* (1998). The human homolog of rat Jagged1 expressed by marrow stroma inhibits differentiation of 32D cells through interaction with Notch1. *Immunity*, **8**, 43–55.

Logeat,F., Bessia,C., Brou,C., Le Bail,O., Jarriault,S., Seidah,N.G. and Israel,A. (1998) The Notch1 receptor is cleaved constitutively by a furin-like convertase. *Proc. Natl Acad. Sci. USA*, **95**, 8108–8112.

Minoguchi,S., Taniguchi,Y., Kato,H., Okazaki,T., Strobl,L.J., Zimber-Strobl,U., Bornkamm,G.W. and Honjo,T. (1997) RBP-L, a transcription factor related to RBP-Jkappa. *Mol. Cell. Biol.*, **17**, 2679–2687.

Morrison,S.J., Perez,S.E., Qiao,Z., Verdi,J.M., Hicks,C., Weinmaster,G. and Anderson,D.J. (2000) Transient Notch activation initiates an irreversible switch from neurogenesis to gliogenesis by neural crest stem cells. *Cell*, **101**, 499–510.

Mumm,J.S., Schroeter,E.H., Saxena,M.T., Griesemer,A., Tian,X., Pan,D.J., Ray,W.J. and Kopan,R. (2000) A ligand-induced extracellular cleavage regulates gamma-secretase-like proteolytic activation of Notch1. *Mol. Cell*, **5**, 197–206.

Oda,T. *et al.* (1997) Mutations in the human Jagged1 gene are responsible for Alagille syndrome. *Nature Genet.*, **16**, 235–242.

Parks,A.L., Klueg,K.M., Stout,J.R. and Muskavitch,M.A. (2000) Ligand endocytosis drives receptor dissociation and activation in the Notch pathway. *Development*, **127**, 1373–1385.

Qi,H., Rand,M.D., Wu,X., Sestan,N., Wang,W., Rakic,P., Xu,T. and Artavanis-Tsakonas,S. (1999) Processing of the notch ligand delta by the metalloprotease Kuzbanian. *Science*, **283**, 91–94.

Rand,M.D., Grimm,L.M., Artavanis-Tsakonas,S., Patriub,V., Blacklow,S.C., Sklar,J. and Aster,J.C. (2000) Calcium depletion dissociates and activates heterodimeric notch receptors. *Mol. Cell. Biol.*, **20**, 1825–1835.

Schroeter,E.H., Kisslinger,J.A. and Kopan,R. (1998) Notch-1 signalling requires ligand-induced proteolytic release of intracellular domain. *Nature*, **393**, 382–386.

Shimizu,K., Chiba,S., Kumano,K., Hosoya,N., Takahashi,T., Kanda,Y., Hamada,Y., Yazaki,Y. and Hirai,H. (1999) Mouse Jagged1 physically interacts with Notch2 and other Notch receptors: Assessment by quantitative methods. *J. Biol. Chem.*, **274**, 32961–32969.

Shimizu,K., Chiba,S., Hosoya,N., Kumano,K., Saito,T., Kurokawa,M., Kanda,Y., Hamada,Y. and Hirai,H. (2000) Binding of Delta1, Jagged1, and Jagged2 to Notch2 rapidly induces cleavage, nuclear translocation, and hyperphosphorylation of Notch2. *Mol. Cell. Biol.*, **20**, 6913–6922.

Struhl,G. and Adachi,A. (1998) Nuclear access and action of notch *in vivo*. *Cell*, **93**, 649–660.

Struhl,G. and Greenwald,I. (1999) Presenilin is required for activity and nuclear access of Notch in *Drosophila*. *Nature*, **398**, 522–525.

Sun,X. and Artavanis-Tsakonas,S. (1996) The intracellular deletions of Delta and Serrate define dominant negative forms of the *Drosophila* Notch ligands. *Development*, **122**, 2465–2474.

Sun,X. and Artavanis-Tsakonas,S. (1997) Secreted forms of DELTA and SERRATE define antagonists of Notch signaling in *Drosophila*. *Development*, **124**, 3439–3448.

Uyttendaele,H., Marazzi,G., Wu,G., Yan,Q., Sassoon,D. and Kitajewski,J. (1996) Notch/Int-3, a mammary proto-oncogene, is an endothelial cell-specific mammalian Notch gene. *Development*, **122**, 2251–2259.

Varnum-Finney,B., Wu,L., Yu,M., Brashem-Stein,C., Staats,S., Flowers,D., Griffin,J.D. and Bernstein,I.D. (2000) Immobilization of Notch ligand, Delta-1, is required for induction of notch signaling. *J. Cell Sci.*, **113**, 4313–4318.

Weinmaster,G. (1997) The ins and outs of notch signaling. *Mol. Cell. Neurosci.*, **9**, 91–102.

Weinmaster,G., Roberts,V. and Lemke,G. (1991) A homolog of *Drosophila* Notch expressed during mammalian development. *Development*, **113**, 199–205.

Weinmaster,G., Roberts,V. and Lemke,G. (1992) Notch2: a second mammalian Notch gene. *Development*, **116**, 931–941.

Ye,Y., Lukinova,N. and Fortini,M.E. (1999) Neurogenic phenotypes and altered Notch processing in *Drosophila* Presenilin mutants. *Nature*, **398**, 525–529.

Received August 10, 2001; revised and accepted December 6, 2001

THE JOURNAL OF BIOLOGICAL CHEMISTRY
Vol. 277, No. 17, Issue of April 26, pp. 14933–14941, 2002
Printed in U.S.A.

MICAL, a Novel CasL Interacting Molecule, Associates with Vimentin*

Received for publication, December 12, 2001
Published, JBC Papers in Press, February 4, 2002, DOI 10.1074/jbc.M111842200

Takahiro Suzuki‡, Tetsuya Nakamoto‡, Seishi Ogawa‡, Sachiko Seo‡, Tomoko Matsumura‡, Kouichi Tachibana§, Chikao Morimoto¶, and Hisamaru Hirai‡‖

From the ‡Department of Hematology and Oncology, Graduate School of Medicine, University of Tokyo, 7-3-1 Hongo, Bunkyo-ku, Tokyo, 113-8655, the §Laboratory of Gene Function Analysis, Institute of Molecular and Cell Biology, National Institute of Advanced Industrial Science and Technology, Central-2 OSL-C2, 1-1-1 Umezono, Tsukuba, Ibaraki 305–8568, and the ¶Department of Clinical Immunology and AIDS Research Center, Institute of Medical Science, University of Tokyo, 4-6-1 Shiroganedai, Minato-ku, Tokyo 108-8639, Japan

CasL/HEF1 belongs to the p130^{Cas} family. It is tyrosine-phosphorylated following β_1 integrin and/or T cell receptor stimulation and is thus considered to be important for immunological reactions. CasL has several structural motifs such as an SH3 domain and a substrate domain and interacts with many molecules through these motifs. To obtain more insights on the CasL-mediated signal transduction, we sought proteins that interact with the CasL SH3 domain by far Western screening, and we identified a novel human molecule, MICAL (a Molecule Interacting with CasL). MICAL is a protein of 118 kDa and is expressed in the thymus, lung, spleen, kidney, testis, and hematopoietic cells. MICAL has a calponin homology domain, a LIM domain, a putative leucine zipper motif, and a proline-rich PPKPP sequence. MICAL associates with CasL through this PPKPP sequence. MICAL is a cytoplasmic protein and colocalizes with CasL at the perinuclear area. Through the COOH-terminal region, MICAL also associates with vimentin that is a major component of intermediate filaments. Immunostaining revealed that MICAL localizes along with vimentin intermediate filaments. These results suggest that MICAL may be a cytoskeletal regulator that connects CasL to intermediate filaments.

CasL (also known as HEF1) was originally identified as a highly phosphorylated protein of 105-kDa in human lymphocytes after β_1 integrin stimulation (1–3). CasL is expressed preferentially in lymphocytes and several epithelial cells. It belongs to the p130^{Cas} (Cas) family that includes Cas, CasL/HEF1, and Efs/Sin (4–6). They contain an SH3 domain at the NH_2 terminus, followed by a substrate domain composed of a cluster of potential SH2-binding sites, and a COOH-terminal domain, which contains consensus binding motifs for the SH3 and SH2 domains of c-Src (CasL does not have binding motifs for c-Src SH3 domain). This structural profile indicates that the Cas family proteins serve as docking molecules that assemble and transduce intracellular signals.

Since Cas was the first characterized member of the Cas family proteins, the study of Cas is most advanced, and it has established a framework for the studies of the other family members. In fibroblasts, Cas has been shown to reside primarily at focal adhesions and along adhesion-proximal regions of stress fibers (7, 8), where Cas associates with focal adhesion kinase (FAK)[1] (9). When cells attach to extracellular matrix proteins such as fibronectin, laminin, or vitronectin through integrin molecules, they form focal adhesion structures (also simply called "focal adhesions") at the adhesion sites. At focal adhesions, stress fibers are tethered, and a variety of molecules that mediate many cellular functions such as proliferation and migration are integrated (10, 11). Cas, localizing at focal adhesions, plays important roles in the integrin-induced signaling. By generating and examining Cas knockout mice, we have demonstrated that Cas is essential for bundling actin filaments and cellular transformation induced by the oncogenic Src (12).

Cytoskeletal system is essential for maintaining various cellular functions. In the mammalian cells, there are three types of cytoskeletal filaments, actin-containing microfilaments, tubulin-containing microtubules, and intermediate filaments (IFs). Among them, IFs are important for structure and mechanical integration of cellular space, and they are composed of cell type-specific proteins (13–17). Vimentin is one of such proteins and is a major component of IFs in cells of mesenchymal tissues.

Recently, an increasing number of studies are reported on the CasL-mediated functions. As suggested by its structural similarity to Cas, CasL is considered to be important for β_1 integrin-induced signal transduction and cytoskeletal regulation (18). In T lymphocytes, CasL also plays a critical role in T cell receptor (TCR)-induced migration (19).

These CasL (or Cas)-mediated functions are carried out by its interaction with many molecules. CasL has several domains that interact with other molecules, such as the SH3 and the substrate domain. The SH3 domain of CasL interacts with FAK or Pyk2/Cakβ/RAFTK/CADTK, and this interaction is considered to be one of the triggers of the signal transduction following β_1 integrin stimulation (3, 20–22). In the case of Cas, however, not only FAK or Pyk2 but also several other molecules such as PTP-1B (23), PTP-PEST (24), C3G (25), and CIZ (26) are demonstrated to interact with its SH3 domain, and they mediate cellular functions. Therefore, there may exist other unknown SH3-binding molecules and pathways in the

* The costs of publication of this article were defrayed in part by the payment of page charges. This article must therefore be hereby marked "*advertisement*" in accordance with 18 U.S.C. Section 1734 solely to indicate this fact.

The nucleotide sequence(s) reported in this paper has been submitted to the GenBank™/EBI Data Bank with accession number(s) AB048948.

‖ To whom correspondence should be addressed: Dept. of Hematology and Oncology, Graduate School of Medicine, University of Tokyo, 7-3-1 Hongo, Bunkyo-ku, Tokyo, 113-8655, Japan. Tel.: 81-3-5800-6421; Fax: 81-3-5689-7286; E-mail: hhirai-tky@umin.ac.jp.

[1] The abbreviations used are: FAK, focal adhesion kinase; SH, Src homology; GST, glutathione S-transferase; IFs, intermediate filaments; TCR, T cell receptor; HA, hemagglutinin; CH, calponin homology; Wt, wild type; mAb, monoclonal antibody; L-Zip, leucine zipper.

A

```
cccaagactgtccccgctggaggcggtagagggatccagaagtaatga/gatgctaatgagtcgcgaa      67
taaagcccgggcggcgccccgcgcccctcgcggaagcccacactccgcgcgactccaggcgcacgccc     135
cgggccgccccgcatcccagcatccccgcccgatctcggcgtttccgcccccgcccccgcccccgccc     203
tcccacccgctcagacctggttgccagcccaacaggaagcggcccctcccggcttcggagccgccgcc     271
actcgtctctgcccagctgctgccctccccaggaggcctccATG GCT TCA CCT ACC TCC ACC AAC  336
                                            M   A   S   P   T   S   T   N    8

CCA GCG CAT GCC CAC TTT GAG AGC TTC CTG CAG GCC CAG CTG TGC CAG GAC GTG CTG AGC  396
P   A   H   A   H   F   E   S   F   L   Q   A   Q   L   C   Q   D   V   L   S   28

AGC TTC CAG GAG CTG TGT GGG GCC CTG GGG CTG GAA CCC GGT GGG GGG CTG CCC CAG TAC  456
S   F   Q   E   L   C   G   A   L   G   L   E   P   G   G   G   L   P   Q   Y   48

CAC AAG ATC AAG GAC CAG CTC AAC TAC TGG AGC GCC AAG TCA CTG TGG ACC AAG CTG GAC  516
H   K   I   K   D   Q   L   N   Y   W   S   A   K   S   L   W   T   K   L   D   68

AAG CGA GCA GGC CAG CCT GTC TAC CAG CAG GGC CGG GCC TGC ACC AGC ACC AAG TGC CTG  576
K   R   A   G   Q   P   V   Y   Q   Q   G   R   A   C   T   S   T   K   C   L   88

GTG GTG GGT GCT GGA CCT TGC GGG CTG CGG GTC GCT GTG GAG CTG GCG CTG CTG GGG GCC  636
V   V   G   A   G   P   C   G   L   R   V   A   V   E   L   A   L   L   G   A  108

CGA GTG GTG CTG GTG GAA AAG CGC ACC AAG TTC TCT CGC CAC AAC GTG CTC CAC CTC TGG  696
R   V   V   L   V   E   K   R   T   K   F   S   R   H   N   V   L   H   L   W  128

CCC TTC ACC ATC CAC GAC CTG CGG GCA CTC GGT GCT AAG AAG TTC TAC GGG CGC TTC TGC  756
P   F   T   I   H   D   L   R   A   L   G   A   K   K   F   Y   G   R   F   C  148

ACC GGC ACC CTG GAC CAC ATC AGC ATC AGG CAG CTC CAG CTG CTT CTG CTG AAG GTA GCA  816
T   G   T   L   D   H   I   S   I   R   Q   L   Q   L   L   L   L   K   V   A  168

TTG CTG CTG GGG GTG GAA ATT CAC TGG GGT GTC ACT TTC ACT GGC CTC CAG CCC CCT CCT  876
L   L   L   G   V   E   I   H   W   G   V   T   F   T   G   L   Q   P   P   P  188

AGG AAG GGG AGT GGC TGG CGT GCC CAG CTC CAA CCC AAC CCC CCT GCC CAG CTG GCC AAC  936
R   K   G   S   G   W   R   A   Q   L   Q   P   N   P   P   A   Q   L   A   N  208

TAT GAA TTT GAC GTC CTT ATC TCG GCT GCA GGA GGT AAA TTC GTC CCT GAA GGC TTC AAA  996
Y   E   F   D   V   L   I   S   A   A   G   G   K   F   V   P   E   G   F   K  228

GTT CGA GAA ATG CGA GGC AAA CTG GCC ATT GGC ATC ACA GCC AAC TTT GTG AAT GGA CGC 1056
V   R   E   M   R   G   K   L   A   I   G   I   T   A   N   F   V   N   G   R  248

ACC GTG GAG GAG ACA CAG GTG CCG GAG ATC AGT GGT GTA GCC AGG ATC TAC AAC CAG AGC 1116
T   V   E   E   T   Q   V   P   E   I   S   G   V   A   R   I   Y   N   Q   S  268

TTC TTC CAG AGC CTT CTC AAA GCC ACA GGC ATT GAT CTG GAG AAC ATT GTG TAC TAC AAG 1176
F   F   Q   S   L   L   K   A   T   G   I   D   L   E   N   I   V   Y   Y   K  288

GAC GAC ACC CAC TAC TTT GTG ATG ACA GCC AAG AAG CAG TGC CTG CTG CGG CTG GGG GTG 1236
D   D   T   H   Y   F   V   M   T   A   K   K   Q   C   L   L   R   L   G   V  308

CTG CGC CAG GAC TGG CCA GAC ACC AAT CGG CTG CTG GGC AGT GCC AAT GTG GTG CCC GAG 1296
L   R   Q   D   W   P   D   T   N   R   L   L   G   S   A   N   V   V   P   E  328

GCT CTG CAG CGC TTT ACC CGG GCA GCT GCT GAC TTT GCC ACC CAT GGC AAG CTC GGG AAA 1356
A   L   Q   R   F   T   R   A   A   A   D   F   A   T   H   G   K   L   G   K  348

CTA GAG TTT GCC CAG GAT GCC CAT GGG CAG CCT GAT GTC TCT GCC TTT GAC TTC ACG AGC 1416
L   E   F   A   Q   D   A   H   G   Q   P   D   V   S   A   F   D   F   T   S  368

ATG ATG CGG GCA GAG AGT TCT GCT CGT GTG CAA GAG AAG CAT GGC GCC CGC CTG CTG CTG 1476
M   M   R   A   E   S   S   A   R   V   Q   E   K   H   G   A   R   L   L   L  388

GGA CTG GTG GGG GAC TGC CTG GTG GAG CCC TTC TGG CCC CTG GGC ACT GGA GTG GCA CGG 1536
G   L   V   G   D   C   L   V   E   P   F   W   P   L   G   T   G   V   A   R  408

GGC TTC CTG GCA GCC TTT GAT GCA GCC TGG ATG GTG AAG CGG TGG GCA GAG GGC GCT GAG 1596
G   F   L   A   A   F   D   A   A   W   M   V   K   R   W   A   E   G   A   E  428

TCC CTA GAG GTG TTG GCT GAG CGT GAG AGC CTG TAC CAG CTT CTG TCA CAG ACA TCC CCA 1656
S   L   E   V   L   A   E   R   E   S   L   Y   Q   L   L   S   Q   T   S   P  448

GAA AAC ATG CAT CGC AAT GTG GCC CAG TAT GGG CTG GAC CCA GCC ACC CGC TAC CCC AAC 1716
E   N   M   H   R   N   V   A   Q   Y   G   L   D   P   A   T   R   Y   P   N  468

CTG AAC CTC CGG GCA GTG ACC CCC AAT CAG GTA CGA GAC CTG TAT GAT GTG CTA GCC AAG 1776
L   N   L   R   A   V   T   P   N   Q   V   R   D   L   Y   D   V   L   A   K  488

GAG CCT GTG CAG AGG AAC AAC GAC AAG ACA GAT ACA GGG ATG CCA GCC ACC GGG TCG GCA 1836
E   P   V   Q   R   N   N   D   K   T   D   T   G   M   P   A   T   G   S   A  508

GGC ACC CAG GAG GAG CTG CTA CGC TGG TGC CAG GAG CAG ACA GCT GGG TAC CCG GGA GTC 1896
G   T   Q   E   E   L   L   R   W   C   Q   E   Q   T   A   G   Y   P   G   V  528

CAC GTC TCC GAT TTG TCT TCC TCC TGG GCT GAT GGG CTA GCT CTG TGT GCC CTG GTG TAC 1956
H   V   S   D   L   S   S   S   W   A   D   G   L   A   L   C   A   L   V   Y  548

CGG CTG CAG CCT GGC CTG CTG GAA CCC TCA GAG CTG CAG GGG CTG GGA GCT CTG GAA GCA 2016
R   L   Q   P   G   L   L   E   P   S   E   L   Q   G   L   G   A   L   E   A  568

ACT GCT TGG GCA CTA AAG GTG GCA GAG AAT GAG CTG GGC ATC ACA CCG GTG GTG TCT GCA 2076
T   A   W   A   L   K   V   A   E   N   E   L   G   I   T   P   V   V   S   A  588

CAG GCC GTG GTA GCA GGG AGT GAC CCA CTG GGC CTC ATT GCC TAC CTC AGC CAC TTC CAC 2136
Q   A   V   V   A   G   S   D   P   L   G   L   I   A   Y   L   S   H   F   H  608

AGT GCC TTC AAG AGC ATG GCC CAC AGC CCA GGC CCT GTC AGC CAG GCC TCC CCA GGG ACC 2196
S   A   F   K   S   M   A   H   S   P   G   P   V   S   Q   A   S   P   G   T  628

TCC AGT GCT GTA TTA TTC CTT AGT AAA CTT CAG AGG ACC CTG CAG CGA TCC CGG GCC AAG 2256
S   S   A   V   L   F   L   S   K   L   Q   R   T   L   Q   R   S   R   A   K  648

GAA AAT GCA GAG GAT GCT GGT GGC AAG AAG CTG CGC TTG GAG ATG GAG GCC GAG ACC CCA 2316
E   N   A   E   D   A   G   G   K   K   L   R   L   E   M   E   A   E   T   P  668

AGT ACT GAG GTG CCA CCT GAC CCA GAG CCT GGT GTA CCC CTG ACA CCC CCA TCC CAA CAC 2376
S   T   E   V   P   P   D   P   E   P   G   V   P   L   T   P   P   S   O   H  688
AGT ACT GAG GTG CCA CCT GAC CCA GAG CCT GGT GTA CCC CTG ACA CCC CCA TCC CAA CAC 2376
S   T   E   V   P   P   D   P   E   P   G   V   P   L   T   P   P   S   O   H  688
```

FIG. 1. **Nucleotide and predicted amino acid sequences of human MICAL and its schematic representation.** *A*, nucleotide and predicted amino acid (*single-letter code*) sequences of human MICAL are presented. Sequence numbers are shown on the *right*. Shown in *lowercase letters* are non-coding regions. Amino acid residues corresponding to the calponin homology domain, the LIM domain, and the putative leucine zipper motif are *underlined* with *single lines*, *bold lines*, and *double lines*, respectively. The *boxed* amino acid residues represent the proline-rich sequence that is responsible for CasL SH3 binding. The "/" in the 5'-side non-coding region indicates the in-frame stop codon, and the *asterisk* indicates the stop codon of the open reading frame. *B*, schematic representation of the human MICAL and the KIAA0750/MICAL-2 molecules. MICAL consists of a calponin homology domain (*CH*), a LIM domain (*LIM*), a proline-rich region (*PR*), and a putative leucine zipper motif (*L-Zip*). KIAA0750/MICAL-2 is a protein composed of 1124 amino acids, and it has homology with MICAL by 65 (NH_2-terminal half) to 35% (COOH-terminal region). Unlike MICAL, MICAL-2 has neither proline rich regions nor L-Zip motifs. The numbers in the scheme indicate amino acid numbers. The *C1* and *C2 lines* indicate regions used for generating polyclonal antisera.

```
CAG GAG GCC GGT GCT GGG GAC CTG TGT GCA CTT TGT GGG GAA CAC CTC TAT GTC CTG GAA   2436
Q  E  A  G  A  G  D  L  C  A  L  C  G  E  H  L  Y  V  L  E                      708

CGC CTC TGT GTC AAC GGC CAT TTC TTC CAC CGG AGC TGC TTC CGC TGC CAT ACC TGT GAG   2496
R  L  C  V  N  G  H  F  F  H  R  S  C  F  R  C  H  T  C  E                      728

GCC ACA CTG TGG CCA GGT GGC TAT GAG CAG CAC CCA GGA GAT GGA CAT TTC TAC TGC CTC   2556
A  T  L  W  P  G  G  Y  E  Q  H  P  G  D  G  H  F  Y  C  L                      748

CAG CAC CTG CCC CAG ACA GAC CAC AAA AAG GAA GGC AGC GAT AGA GGC CCT GAG AGT CCG   2616
Q  H  L  P  Q  T  D  H  K  K  E  G  S  D  R  G  P  E  S  P                      768

GAG CTC CCC ACA CCA AGT GAG AAT AGC ATG CCA CCA GGC CTC TCA ACT CCC ACA GCC TCG   2676
E  L  P  T  P  S  E  N  S  M  P  P  G  L  S  T  P  T  A  S                      788

CAG GAG GGG GCC GGT CCT GTT CCA GAT CCC AGC CAG CCC ACC CGT CGG CAG ATC CGC CTC   2736
Q  E  G  A  G  P  V  P  D  P  S  Q  P  T  R  R  Q  I  R  L                      808

TCC AGC CCG GAG CGC CAG CGG TTG TCC TCC CTT AAC CTT ACC CCT GAC CCG GAA ATG GAG   2796
S  S  P  E  R  Q  R  L  S  S  L  N  L  T  P  D  P  E  M  E                      828

CCT CCA CCC AAG CCT CCC CGC AGC TGC TCC GCC TTG GCC CGC CAC GCC CTG GAG AGC AGC   2856
P  P  P  K  P  P  R  S  C  S  A  L  A  R  H  A  L  E  S  S                      848

TTT GTG GGC TGG GGC CTG CCA GTC CAG AGC CCT CAA GCT CTT GTG GCC ATG GAG AAG GAG   2916
F  V  G  W  G  L  P  V  Q  S  P  Q  A  L  V  A  M  E  K  E                      868

GAA AAA GAG AGT CCC TTC TCC AGT GAA GAG GAA GAA GAA GAT GTG CCT TTG GAC TCA GAT   2976
E  K  E  S  P  F  S  S  E  E  E  E  D  V  P  L  D  S  D                      888

GTG GAA CAG GCC CTG CAG ACC TTT GCC AAG ACC TCA GGC ACC ATG AAT AAC TAC CCA ACA   3036
V  E  Q  A  L  Q  T  F  A  K  T  S  G  T  M  N  N  Y  P  T                      908

TGG CGT CGG ACT CTG CTG CGC CGT GCG AAG GAG GAG GAG ATG AAG AGG TTC TGC AAG GCC   3096
W  R  R  T  L  L  R  R  A  K  E  E  E  M  K  R  F  C  K  A                      928

CAG ACC ATC CAA CGG CGA CTA AAT GAG ATT GAG GCT GCC TTG AGG GAG CTA GAG GCC GAG   3156
Q  T  I  Q  R  R  L  N  E  I  E  A  A  L  R  E  L  E  A  E                      948

GGC GTG AAG CTG GAG CTG GCC TTG AGG CGC CAG AGC AGT TCC CCA GAA CAG CAA AAG AAA   3216
G  V  K  L  E  L  A  L  R  R  Q  S  S  S  P  E  Q  Q  K  K                      968

CTA TGG GTA GGA CAG CTG CTA CAG CTC GTT GAC AAG AAA AAC AGC TTG GTG GCT GAG GAG   3276
L  W  V  G  Q  L  L  Q  L  V  D  K  K  N  S  L  V  A  E  E                      988

GCC GAG CTC ATG ATC ACG GTG CAG GAA TTG AAT CTG GAG GAG AAA CAG TGG CAG CTG GAC   3336
A  E  L  M  I  T  V  Q  E  L  N  L  E  E  K  Q  W  Q  L  D                     1008

CAG GAG CTA CGA GGC TAC ATG AAC CGG GAA GAA AAC CTA AAG ACA GCT GCT GAT CGG CAG   3396
Q  E  L  R  G  Y  M  N  R  E  E  N  L  K  T  A  A  D  R  Q                     1028

GCT GAG GAC CAG GTC CTG AGG AAG CTG GTG GAT TTG GTC AAC CAG AGA GAT GCC CTC ATC   3456
A  E  D  Q  V  L  R  K  L  V  D  L  V  N  Q  R  D  A  L  I                     1048

CGC TTC CAG GAG GAG CGC AGG CTC AGC GAG CTG GCC TTG GGG ACA GGG GCC CAG GGC TAG   3516
R  F  Q  E  E  R  R  L  S  E  L  A  L  G  T  G  A  Q  G  *                     1067

acgagggtgggccgtctgctttcgttcccacaaagaaagcacctcaccccagcacagtgccacccctg            3584
ttcatctgggctgcctggcagagagccttgctgtttacaattaaaatgtttctgccccaaaaaaaaaa            3652
aaaaaaaaaaaaaaaaaaaaaaaaaaaaaaaaaaaaaaaaaaaaaaaaaaaaaa                          3697
```

FIG. 1—*continued*

B

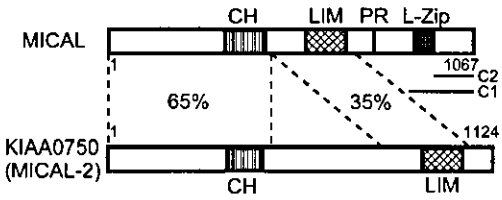

CasL-mediated signal transduction. With this point of view, we sought molecules that interact with the CasL SH3 domain by far Western screening, and we identified a novel molecule that interacts with CasL. We also found that this molecule associates with vimentin and that it could be a regulational component of vimentin filaments.

EXPERIMENTAL PROCEDURES

Cells and Reagents—The human T cell lines H9, Jurkat, and other hematopoietic cell lines HL60 and HEL cells were cultured in RPMI 1640 containing 10% heat-inactivated fetal calf serum. COS7, HeLa, and 293 cells were cultured in Dulbecco's modified Eagle's medium with 10% fetal calf serum.

Rabbit antisera against MICAL C1 and C2 were obtained as described below. Polyclonal antibodies were purified from these antisera by affinity chromatography (HiTrap NHS-activated, Amersham Biosciences, described below). Mouse monoclonal antibody (mAb) V9 against vimentin and mAb M2 against the FLAG epitope were purchased from Sigma. Rabbit polyclonal antibody HA.11 against the hemagglutinin (HA) epitope was obtained from Babco. Goat polyclonal antibodies C-20 against vimentin and N-17 against CasL/HEF1 were purchased from Santa Cruz Biotechnology. The mAb 9E10 against the Myc epitope was obtained by culturing 9E10 hybridomas in the non-serum culture system. Fluorescein isothiocyanate-conjugated anti-rabbit donkey antibody and Texas Red-conjugated anti-goat donkey antibody were purchased from The Jackson Laboratories. The human thymus 5′-STRETCH PLUS cDNA library (HL5010b) was purchased from CLONTECH and was used in the far Western screening.

Far Western Screening—The cDNA fragment encoding the human CasL SH3 domain (amino acid residues 2–66) was generated by PCR using customized primers. *Bgl*II and *Eco*RI sites were added to the 5′- and 3′-ends and subcloned into the *Bam*HI/*Eco*RI sites of pGEX-2TK (Amersham Biosciences) to generate pGEX2TK-CasL SH3. This plasmid was transfected into *Escherichia coli* cells, and the expressed proteins were purified using the glutathione-Sepharose 4B beads (Amersham Biosciences). They were labeled with ^{32}P isotope by bovine heart kinase (Sigma) and used as the first probe.

Competent *E. coli* cells were infected with phages from the cDNA library (20,000 plaque-forming units/plate) and were incubated for 3 h at 43 °C. Then the Hybond-C-extra membranes (Amersham Biosciences) soaked in 10 mM isopropyl-1-thio-β-D-galactopyranoside were overlaid on phage plaques for 4 h at 37 °C, and these membranes were blocked in TBST buffers (10 mM Tris-HCl (pH 8.0), 150 mM NaCl, 0.05% Tween 20) containing 5% skim milk. The membranes were incubated with 0.75 μg of the isotope-labeled GST-CasL SH3 probe for 2 h at 25 °C, washed, and then autoradiographed (Eastman Kodak Co.).

Screening of a PAC Library and a Radiation Hybrid Panel Containing MICAL Gene—To obtain a genomic fragment containing the *MICAL* gene, a PAC library, RPCI-1 (Roswell Park Cancer Institute) was

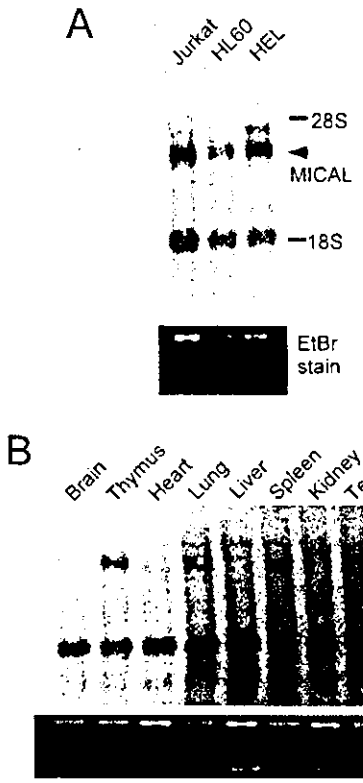

FIG. 2. **Expression profiles of MICAL mRNA.** *A*, Northern blot analysis of the poly(A) RNA from several hematopoietic cell lines. The electrophoresed poly(A) RNA was hybridized with the ^{32}P-labeled MICAL cDNA clone initially isolated in the far Western screening. There is a discrete band at ~3.7 kb (*arrowhead*). This probe cross-reacts with the 18 S rRNA. The ethidium bromide (*EtBr*) staining of the electrophoresed RNA is shown in the *lower panel*. *B*, Northern blot analysis of the poly(A) RNA from adult murine tissues hybridized by the same MICAL cDNA probe. MICAL mRNA is detected in the thymus, lung, spleen, kidney, and testis (*arrowhead*).

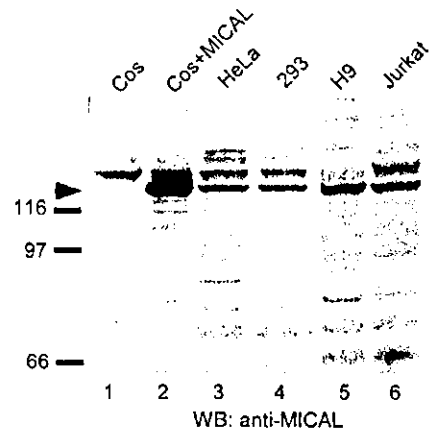

FIG. 3. **Detection of the MICAL proteins.** Cell lysates from COS7 (*lane 1*), COS7 transfected with pSSRα/MICAL (*lane 2*), HeLa (*lane 3*), 293 (*lane 4*), H9 (*lane 5*), and Jurkat (*lane 6*) cells were subjected to immunoblotting with affinity-purified anti-MICAL C2 antibody. MICAL is detected as a single band of ~120 kDa (*arrowhead*). In the COS7 cells transfected with pSSRα/MICAL, prominent expression can be detected. *WB*, Western blot.

screened by the PCR method with a pair of MICAL cDNA-specific primers, P1 and P2 (described below), and we obtained clone 231G18.

To identify the chromosomal location of the *MICAL* gene, we screened a Radiation Hybrid Panel, GeneBridge 4 (Research Genetics), by PCR with the same primers P1 and P2. The results were analyzed by the manufacturer.

Reverse Transcriptase-PCR—Total RNA was extracted from freshly prepared H9 cells by the acid guanidine/phenol chloroform method, and a poly(A) RNA-rich fraction was prepared by the poly(A) selection procedure (Oligotex-dT30 super, Roche Molecular Biochemicals). This RNA fraction was subjected to reverse transcription reaction with a gene-specific primer P3 by heat-resistant reverse transcriptase (Thermoscript, Invitrogen) at 62 °C. We carried out the first PCR on this synthesized cDNA with primers P4 and P6 followed by the second PCR with primers P5 and P6 at the presence of 5% Me_2SO.

The following *MICAL* gene-specific primers were used: P1, CTGCCCCAGTACCACAAGAT (corresponding to nucleotides 445–464); P2, GAGAACTTGGTGCGCTTTTC (nucleotides 652–671); P3, AGGTGGAGCACGTTGTGGCGAGAG (nucleotides 669–692); P4, CCCAAGACTGTCCCCGCTGGAG (nucleotides 1–22); P5, GCTGGAGGCGGTAGAGGGAT (nucleotides 16–35); and P6, CAGCAGCTGGGCAGAGACGAGT (nucleotides 272–293).

Northern Blotting—A poly(A) RNA fraction was obtained from freshly prepared murine tissues or cultured cells as described above. Two μg of this RNA fraction was loaded, electrophoresed, and hybridized with the isotope-labeled MICAL cDNA fragment.

Generation of Antibodies against Bacterially Expressed MICAL—The cDNA fragments corresponding to the amino acid residues 884–1063 (C1) and 999–1063 (C2) of MICAL were generated by PCR, and they were inserted into pGEX1 (Amersham Biosciences) to generate GST-MICAL C1 and GST-MICAL C2 constructs. These plasmids were transfected into *E. coli* cells, and expressed fusion proteins were purified. Rabbits were immunized with these fusion proteins, and antisera against these antigens were raised (anti-MICAL C1 and anti-MICAL C2). The antisera were purified by affinity chromatography. At first, the antisera were passed through the GST-conjugated column removing anti-GST antibodies. The flow-through fraction was then applied onto the antigen-conjugated column, and specific antibodies bound to the column were eluted out and collected.

Plasmid Construction of Expressing Vectors and Transient Transfection—The cDNA for HA tag or FLAG tag was added to the 3′ terminus of the coding sequence of MICAL, and this was inserted into pUC-CAGGS (27) or pSSRαbsr (28) vectors, generating pUC-CAGGS/MICAL-HA and pSSRαbsr/MICAL-FLAG. To make mMICAL mutant, the cDNA sequence CCACCCAAGCCT (corresponding to amino acid sequence PPKP) was mutated to CCACCGGCGCCT (PPAP) by *in vitro* mutagenesis with the Chameleon Double-stranded, Site-directed Mutagenesis Kit (Stratagene). The FLAG tag sequence was added to its 3′ terminus, and mMICAL-FLAG was inserted into the pSSRαbsr vector. To generate M1, M2, M3, and M4 mutants, cDNA fragments corresponding to each mutant protein were generated by PCR using specific primers, and the M5 mutant was generated by PCR-based mutagenesis (ExSite PCR-based Site-directed Mutagenesis Kit, Stratagene). Generated cDNA fragments were ligated with the HA tag sequence, and they were inserted into the pSSRαbsr vector. The generation of c-Myc-tagged CasL was described previously (20). To generate the FLAG-tagged vimentin expression vector, the FLAG tag sequence was ligated to the end of the murine vimentin sequence, and this DNA fragment was inserted into the pUC-CAGGS vector.

These expression vectors were transfected into COS7 cells by the DEAE-dextran method essentially as described previously (29).

Cell Lysis, Immunoprecipitation, and Immunoblotting—Cells were lysed in 1% Triton X-100 buffer (10 mM Tris-HCl (pH 7.4), 5 mM EDTA, 150 mM NaCl, 1% Triton X-100). Cell lysates were incubated with indicated antibodies for 1 h at 4 °C, followed by additional incubation with the protein A- or protein G-Sepharose beads (Amersham Biosciences). The beads were washed with 1% Triton X-100 buffer and treated with sample buffer (2% SDS, 10% glycerol, 60 mM Tris-HCl (pH 6.8), 0.001% bromphenol blue). Samples were subjected to SDS-PAGE. The electrophoresed proteins were transferred to polyvinylidene difluoride filters (Millipore) and were subjected to immunoblotting, followed by detection with the alkaline phosphatase-conjugated secondary antibody (Promega).

Immunofluorescence Microscopy—Cells were grown on a cover glass. They were fixed with 3.7% formaldehyde and permeabilized with 0.2% Triton X-100, and they were blocked in phosphate-buffered saline with 1% bovine serum albumin (Nacalai Tesque, Kyoto, Japan). After incubation with the primary and the secondary antibodies for 1 h at room temperature, the samples were mounted in a 1:1 mixture of 2.5% 1,4-diazabicyclo[2.2.2]octane (Sigma) in phosphate-buffered saline and glycerol. The cells were observed under the MRC1024 confocal microscopic system (Bio-Rad).

In Vitro Pull-down Assay—For pull-down assay, expressed GST fusion proteins were incubated with the glutathione-Sepharose 4B beads (Amersham Biosciences) for 1 h at 4 °C for immobilization. We prepared

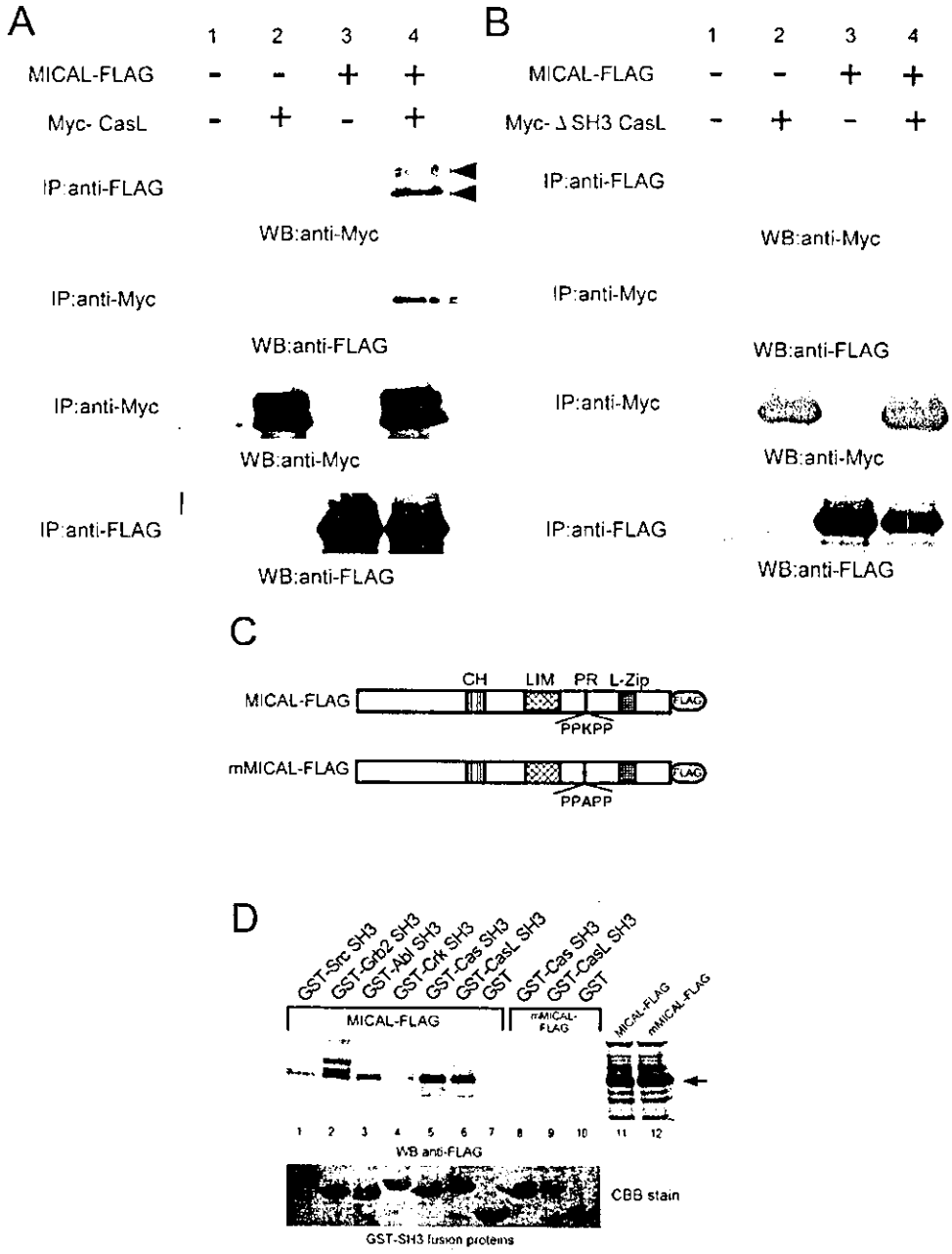

FIG. 4. **MICAL and CasL associate with each other through their PPKPP sequence and SH3 domain, respectively.** *A*, COS7 cells were transiently transfected with the MICAL-FLAG and/or the Myc-CasL expression vectors, and cell lysates were immunoprecipitated (*IP*) with the anti-FLAG or the anti-Myc antibodies. In the cells transfected with both constructs (*lane 4*), CasL was detected in the anti-FLAG immunoprecipitate (*black arrowheads*), and MICAL was detected in the anti-Myc immunoprecipitate (*white arrowhead*). *B*, COS7 cells were transiently transfected with the MICAL-FLAG and/or the Myc-ΔSH3 CasL expression vectors, and cell lysates were immunoprecipitated with the anti-FLAG or the anti-Myc antibodies. We could find neither ΔSH3 CasL in the anti-FLAG immunoprecipitate nor MICAL in the anti-Myc immunoprecipitate (*lane 4*). *C*, schematic representation of the MICAL-FLAG and the mutated MICAL-FLAG (mMICAL-FLAG) molecules. In the mMICAL-FLAG molecule, the single lysine residue in the proline-rich region is replaced by alanine. *D*, several GST-SH3 fusion proteins were incubated with cell lysates containing MICAL-FLAG or mMICAL-FLAG, and they were subjected to immunoblotting. MICAL was clearly detected (*arrow*) in the complexes containing the GST-CasL SH3 (*lane 6*) and the GST-Cas SH3 (*lane 5*) fusion proteins. However, only faint volume of MICAL was found in the complexes containing the GST-Src SH3 (*lane 1*), GST-Grb2 SH3 (*lane 2*), GST-Abl SH3 (*lane 3*), and GST-Crk SH3 (*lane 4*) fusion proteins. In the mMICAL-FLAG lysate, no complex formation was detectable (*lanes 8–10*). In *lanes 11* and *12*, total cell lysates containing MICAL- and mMICAL-FLAG were loaded. *Lower panel* shows the Coomassie Brilliant Blue staining of the GST-SH3 fusion proteins. This shows that almost equal volume of GST fusion proteins were loaded in the reaction. *WB*, Western blot.

aliquots of cell lysates from COS7 cells transfected with MICAL and mMICAL constructs, and these aliquots were incubated with the beads for 1 h, and the proteins bound to the beads were analyzed by immunoblotting. Ten percent of the immobilized proteins were subjected to Coomassie Brilliant Blue stain, and we confirmed that an almost equal volume of GST fusion proteins was loaded. The GST-p130^{Cas} SH3 fusion protein encodes amino acid residues 6–64 of p130^{Cas}. The details of the GST-Crk SH3, GST-Abl SH3, GST-Grb2 SH3, and GST-Src SH3 constructs were described previously (29).

RESULTS

Isolation and Structure Analysis of MICAL—Isotope-labeled GST-CasL SH3 fusion protein was used as a probe for the far Western screening to screen a λgt11 cDNA expression library (CLONTECH) that was derived from normal human thymuses. Approximately 1.5 million phages were screened, and we obtained 8 discrete positive clones. Among them, one clone was

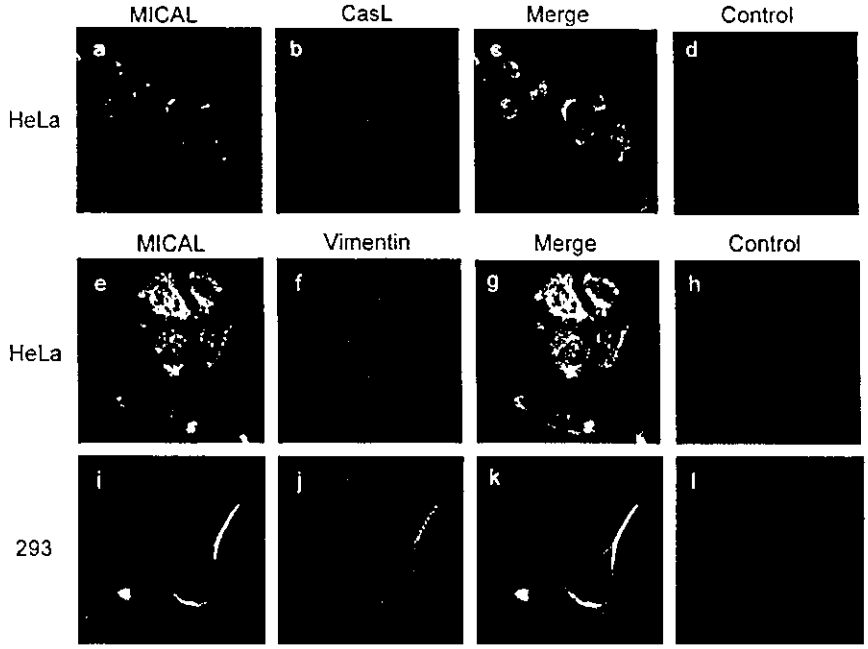

FIG. 5. **MICAL localizes in the cytoplasm and colocalizes with CasL and vimentin.** Cells were costained with the purified anti-MICAL C2 antibody and the anti-CasL/HEF1 or the anti-vimentin antibodies. In HeLa cells, MICAL localizes in the cytoplasm-like filaments or meshes, and this filamentous structure spreads from the perinuclear area toward the cell periphery (*a* and *e*). Similarly, CasL localizes all over the cytoplasm, and it is distributed preferably to the perinuclear area and the cell periphery (*b*). In the merged image, *yellow* colocalization signal is readily detected at the perinuclear area (*c*). In HeLa cells, vimentin is found in the cytoplasm as filamentous or mesh-like structures (*f*), and this localization pattern clearly overlaps with that of MICAL (*g*, *yellow* signal). This colocalization was most clear in 293 cells (*i*, *j*, and *k*). When cells were stained only with the second antibodies, no significant signals were observed (*d*, *h*, and *l*).

identified as FAK, one as PTP-1B, two clones as PTP-PEST, and two as C3G; these molecules have already been known to interact with the Cas SH3 domain (9, 23–25). The other two clones contained an overlapping part of the same unknown gene. To obtain more information on this unknown gene, we continued serial screening procedures using the identified cDNA fragments as probes by the DNA hybridization method. Consequently, we could obtain one conceptional cDNA sequence. However, as the deduced start codon (ATG) of this cDNA did not meet the "Kozak's rule" (30) optimally, we searched for a potential upstream coding region. We screened a PAC genomic library, and obtained a PAC clone, RPCI-1 231G18, that harbored this unknown gene. Sequence analysis of this genomic fragment revealed that an intron sequence was inserted between the cDNA nucleotide 268 and 269 (Fig. 1*A*), and we obtained an additional 5′-side genomic nucleotide sequence. To examine if this 5′-side genomic region is transcribed into mRNA, we prepared three kinds of primers, P4, P5, and P6 (described under "Experimental Procedures"), and we carried out reverse transcriptase-PCR for the mRNA extracted from the human T lymphocyte cell line, H9. Because the nucleotide component around the target region was extremely GC-rich, we carried out reverse transcription at 62 °C with thermoresistant reverse transcriptase. Then we performed the first PCR with P4 and P6 primers and the second PCR with P5 and P6 primers in the presence of 5% Me_2SO. Consequently, we obtained an amplified fragment at the size of ~280 bp, and the sequence analysis of this fragment revealed that this fragment did not contain any intron sequences. These results suggest that this amplified fragment was derived from mRNA and that it was a part of the cDNA. Because this cDNA sequence contained an in-frame stop codon at the nucleotide 48 (Fig. 1*A*), we concluded that we obtained the full-length coding region of this unknown gene.

The cDNA of this newly isolated gene consists of ~3700-bp nucleotides, which corresponds to the result of the Northern blotting described below. Molecular mass of the translated protein is predicted to be 118 kDa composed of 1067 amino acids. Search of the GenBank™ data base showed that this isolated gene encodes a novel molecule, and its amino acid sequence has prominent homology with that of KIAA0750 (35~65% homology) which had been isolated from the human brain (Fig. 1*B*) (31). This data base also told us that MICAL has homology with KIAA1364 derived from human brain by 50–63%. At present, the complete cDNA sequence of KIAA1364 is not determined.

Sequence analysis of this novel molecule indicates that it contains a calponin homology (CH) domain in the central region followed by a LIM domain. In addition, a proline-rich region (Pro-Pro-Lys-Pro-Pro, PPKPP) and a putative leucine zipper (L-Zip) motif are located at the COOH terminus. Because this novel molecule interacts with CasL (described below), we named this novel molecule "MICAL," for a Molecule Interacting with CasL. We also call the KIAA0750 molecule "MICAL-2" based on its homology. Whereas the MICAL-2/KIAA0750 molecule has a CH domain and a LIM domain, it does not have any L-Zip motifs or PPKPP sequences.

To determine the chromosomal location of the *MICAL* gene, we screened a Radiation Hybrid Panel following the manufacturer's instruction. The result showed that *MICAL* is located on the long arm of chromosome 6, 6q16.

MICAL Is Expressed in Hematopoietic Cells and Other Specific Tissues—To assess the expression profile of the MICAL mRNA, we examined various hematopoietic cell lines and murine tissues by Northern blotting. We detected a single discrete transcript of ~3.7 kb in the hematopoietic cell lines Jurkat, HL60, and HEL (Fig. 2*A*). Although we could find another larger transcript in HEL cells, the main transcript was ~3.7 kb. Northern blotting of the various murine tissues revealed that MICAL mRNA expression is restricted to the several specific tissues; we could find prominent expression in the thymus, lung, spleen, and testis and faint expression in the kidney (Fig. 2*B*), whereas no obvious expression was detected in the brain, heart, and liver. Even though the size of the transcript in the testis seemed to be slightly larger than 3.7 kb, this may be a spliced variant.

It has been reported that CasL is expressed prominently in the lung, kidney, placenta, and lymphocytes (2, 3). The expression pattern of MICAL corresponds to that of CasL, and this accordance supports the biological relationship between the two molecules.

Generation of Polyclonal Antibodies and Detection of MICAL Proteins—To characterize MICAL protein, we generated polyclonal antibodies against MICAL. We used COOH-terminal

regions as immunogens, C1 region spanning amino acid residues 884–1063 and C2 region spanning residues 999–1063. We immunized rabbits and obtained antisera to each antigen (anti-MICAL C1 and anti-MICAL C2). The antisera were purified by affinity chromatography, and we generated specific antibodies. To check the quality of these antibodies and to detect MICAL proteins, we performed an immunoblot assay. We used lysates from COS7 cells transiently transfected with pSSRαbsr/MICAL and lysates from normally growing HeLa, 293, H9, and Jurkat cells. By using both antibodies, we could find endogenous expression of MICAL at the size of ~120 kDa in the HeLa, 293, H9, and Jurkat cells and prominent expression in the transfected COS7 cells (Fig. 3).

MICAL Interacts with the CasL SH3 Domain through the PPKPP Proline-rich Sequence—To test the *in vivo* interaction between MICAL and CasL, we analyzed their interaction by transiently coexpressing MICAL and CasL proteins in COS7 cells. When we cotransfected the FLAG-tagged MICAL (MICAL-FLAG) together with the Myc-tagged CasL (Myc-CasL), we could detect CasL in the anti-FLAG immunoprecipitates containing MICAL proteins (Fig. 4*A*). Alternatively, we were able to find MICAL in the anti-Myc immunoprecipitates containing CasL proteins (Fig. 4*A*). These results indicate that these two proteins can make a complex in mammalian cells *in vivo*.

To confirm that MICAL and CasL interact with each other through the CasL SH3 domain, we cotransfected MICAL-FLAG together with the Myc-tagged CasL whose SH3 domain was deleted (Myc-ΔSH3 CasL) and performed immunoprecipitation. In this experiment, we could not find Myc-ΔSH3 CasL in the anti-FLAG immunoprecipitates nor MICAL-FLAG in the anti-Myc immunoprecipitates (Fig. 4*B*). This result indicates that MICAL and CasL interact through the CasL SH3 domain.

This interaction was also demonstrated by the *in vitro* pull-down assay. We immobilized various GST-SH3 fusion proteins on the glutathione-Sepharose beads and incubated them with COS7 cell lysates expressing MICAL-FLAG. As shown in Fig. 4*D*, we could detect prominent existence of MICAL in the complex that contains the CasL SH3 domain or Cas SH3 domain, whereas only faint MICAL bands were observed in the Src SH3, Grb2 SH3, Abl SH3, or Crk SH3 containing complex. This result shows that MICAL preferentially interacts with the CasL (or $p130^{Cas}$) SH3 domain.

It has been reported that the Cas SH3 domain preferentially binds to "Pro-*X*-Lys-Pro, PXKP" (*X*, any amino acid) sequence (25). Because MICAL has a consensus sequence of "PPKPP" at the COOH terminus, we examined whether MICAL interacts with the CasL SH3 domain through this proline-rich sequence. We constructed a mutant, mMICAL-FLAG, whose proline-rich sequence PPKPP (amino acid residues 830–834) was mutated into PPAPP (Fig. 4*C*). When we incubated the immobilized GST-CasL SH3 and GST-Cas SH3 fusion proteins with lysates of COS7 cells expressing mMICAL-FLAG, we could not find mMICAL proteins in the complexes (Fig. 4*D*). These results indicate that MICAL interacts with the CasL and Cas SH3 domains through the PPKPP sequence.

MICAL Is a Cytoplasmic Protein and Colocalizes with CasL at the Perinuclear Region—To examine the intracellular distribution of the MICAL molecule, we performed immunofluorescence staining with the purified anti-MICAL C2 antibody. MICAL localized in the cytoplasm like filaments or meshes, and this filamentous structure spread from the perinuclear area toward the cell periphery (Fig. 5, *a* and *e*). When we stained the CasL molecule, CasL also localized all over the cytoplasm but distributed preferentially to the perinuclear area and the edge of the cell periphery (Fig. 5*b*). We could readily find the colocalization signals of MICAL and CasL at the perinuclear area (Fig. 5*c*). These results suggest that there are biological interactions between MICAL and CasL in living cells.

MICAL Also Colocalizes with Vimentin Intermediate Filaments—MICAL is distributed in the cytoplasm-like filaments in HeLa cells. Because this staining pattern was similar to that of cytoskeletal structures, we examined subcellular localization of microfilaments (F-actin), microtubules (α-tubulin), or intermediate filaments (vimentin) by costaining these cytoskeletal molecules with MICAL. Double staining of these proteins revealed that the staining pattern of MICAL was mostly consistent with that of vimentin (Fig. 5, *middle panel*). This colocalization pattern was more apparent in 293 cells; MICAL was stained like mesh composed of fine filaments in the cytoplasm, and in many cells, strong signals were observed in the cell process areas (Fig. 5, *lower panel*). Therefore, MICAL was supposed to be an integrated component of vimentin intermediate filaments.

MICAL Associates with Vimentin through Its COOH-terminal Region—To examine the possible interaction between MICAL and vimentin, we performed immunoprecipitation and immunoblotting. Prior to these experiments, we generated five deletion mutants of MICAL, M1–M5 (Fig. 6*A*). At first, we transfected COS7 cells with these mutants or wild-type (Wt) MICAL-HA constructs, and the cell lysates were subjected to immunoprecipitation with the anti-vimentin antibody. In this experiment, we could find M3–M5 and Wt molecules in the anti-vimentin immunoprecipitates (Fig. 6*B*, *lanes 8–10* and *13*), whereas M1 and M2 mutants were not found in these immunocomplexes (Fig. 6*B*, *lanes 3* and *4*). This result indicates that MICAL interacts with vimentin through its COOH-terminal region.

To confirm this interaction between MICAL and vimentin, we cotransfected COS7 cells with FLAG-tagged vimentin and MICAL M2 or Wt constructs, and the cell lysates were immunoprecipitated with the anti-HA antibody. As a result, we identified the Wt molecule in the anti-FLAG immunoprecipitate (Fig. 6*C*, *lane 5*), whereas M2 molecule was not found in the complex (Fig. 6*C*, *lane 4*).

These results clearly show that MICAL and vimentin make complexes in living cells and that this interaction is mediated through the COOH-terminal region of MICAL.

DISCUSSION

In this study, we identified a novel molecule, MICAL, as a potential CasL-interacting protein by far Western screening. MICAL is preferentially expressed in hematopoietic cells and several specific tissues. MICAL contains some discrete domains that include a CH domain, a LIM domain, and a proline-rich motif. We cannot predict any enzymatically functional domains from its primary sequence.

SH3 domains bind proline-rich motifs with the core consensus sequence P*X*X*P* (32). Amino acid residues immediately adjacent to the proline residues seem to be significant for binding specificity to different SH3 domains (33, 34). Several consensus sequences binding to the Cas SH3 domain have been reported, and one of them is PPKPP (25). MICAL has this sequence at the COOH terminus, and we demonstrated their *in vivo* interaction. Moreover, in this screening, we identified other molecules, PTP-1B, PTP-PEST, FAK, and C3G, as CasL SH3-binding partners. These molecules have already been shown to interact with the Cas SH3 domain (9, 23–25). Because the SH3 domain of Cas and that of CasL have amino acid homology by more than 80%, this similarity in their binding partners seems reasonable.

CasL is a molecule that belongs to the Cas family and is important for TCR- and β_1 integrin-induced immunological

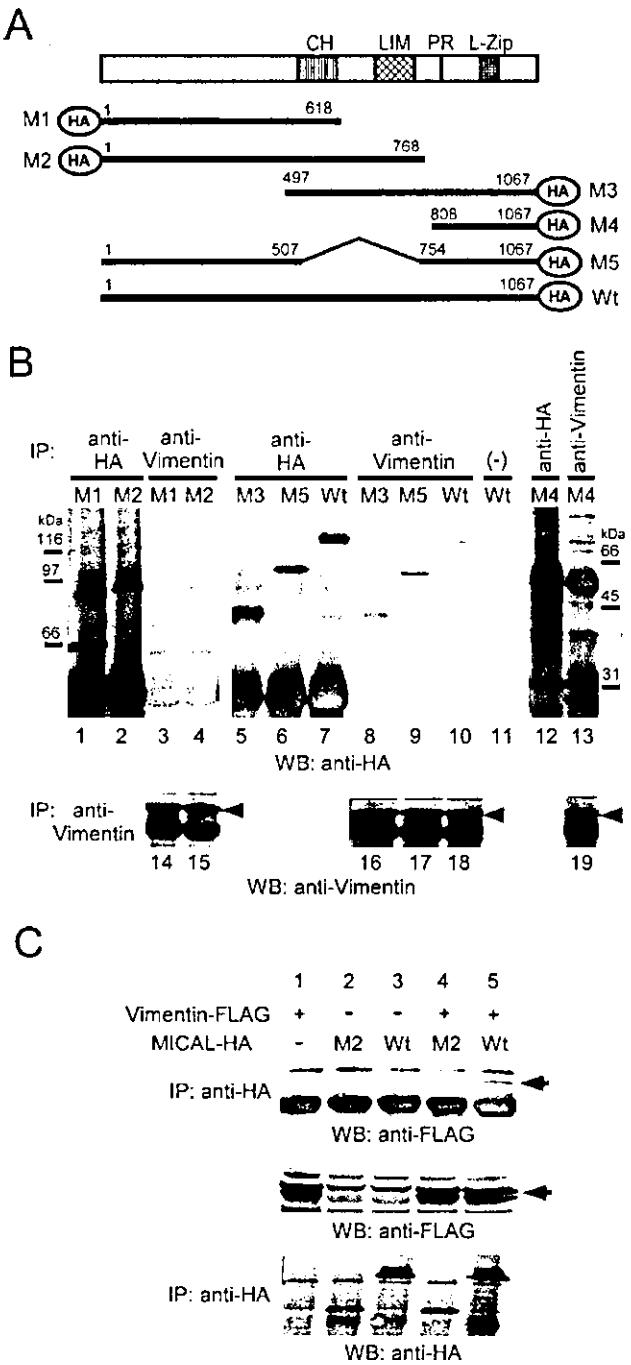

FIG. 6. **MICAL interacts with vimentin molecule through its COOH-terminal region.** *A*, schematic representation of the MICAL-HA mutants. Five HA-tagged mutants (*M1–M5*) and an HA-tagged wild-type MICAL (Wt) construct were generated. *M1*, NH_3-terminal fragment to the CH domain; *M2*, NH_3-terminal fragment to the LIM domain; *M3*, COOH-terminal fragment from the CH domain; *M4*, COOH-terminal fragment from the end of the LIM domain; *M5*, fragment from which the CH domain and the LIM domain are deleted. *Numbers* on the *lines* represent corresponding amino acid numbers. *B*, COS7 cells were transiently transfected with expression vectors encoding HA-tagged mutants, and cell lysates were subjected to immunoprecipitation (*IP*) with the anti-HA or the anti-vimentin antibodies. *M3–M5* and *Wt* proteins were detected in the anti-vimentin immunoprecipitates (*lanes 8, 13, 9,* and *10*), whereas M1 and M2 mutants were not found in the anti-vimentin immunoprecipitates (*lanes 3* and *4*). No Wt proteins were found in the fraction nonspecifically bound to the protein G-Sepharose (*lane 11*). *Lanes 1, 2, 5–7,* and *12* show expressed HA-tagged proteins, and *black arrowheads* in the *lower panel* point at the vimentin proteins in the immunoprecipitates (*lanes 14–19*). The *white arrowhead* in the *lanes 12* and *13* indicates the M4 mutant. *C*, COS7 cells were transiently transfected with HA-tagged MICAL mutants (*Wt* or *M2*) and/or FLAG-tagged vimentin (*Vim*) expression vectors, and cell lysates were subjected to immunoprecipitation with the anti-HA antibody. In the cells transfected with Wt and vimentin (*lane 5*), vimentin was detected in the anti-HA immunoprecipitate (*upper panel, black arrow*), whereas in the cells expressing M2 and vimentin (*lane 4*), vimentin was not identified in the anti-HA immunoprecipitate. In the cells transfected with vimentin, M2, or M3 alone (*lanes 1–3*), we could not find any vimentin signals in the anti-HA immunoprecipitates. The *black arrow* in the *middle panel* indicates the expressed vimentin proteins (*lanes 1, 4,* and *5*), and the *lower panel* shows the expression of Wt (*lanes 3* and *5*) or M2 (*lanes 2* and *4*) proteins. *WB*, Western blot.

reactions such as interleukin-2 production (35) and migratory response (19). In HeLa cells, CasL localizes around the nucleus and at the cell periphery. Various reports have suggested that the Cas family proteins transduce signals to downstream pathways including mitogen-activated protein kinase and other cytoskeletal regulatory pathways (12, 18, 19, 36–38). In this report, we showed that a fraction of MICAL localizes at the perinuclear area and colocalizes with CasL. This result suggests that MICAL may play roles in the CasL-mediated signaling pathways.

In lymphocytes, ligation of TCR, B cell receptor, or β_1 integrin induces prominent phosphorylation of CasL at its substrate domain. This is considered to be important for many immunological reactions (19, 21, 22, 35, 39). Therefore, we examined whether MICAL could be phosphorylated at tyrosine residues after TCR or β_1 integrin ligation. However, we could not find any obvious tyrosine phosphorylation (data not shown). MICAL may not be a target of phosphorylation by tyrosine kinases.

In addition to the interaction with CasL, we demonstrated that MICAL associates with vimentin molecules and colocalizes with vimentin IFs *in vivo*. In mammalian cells, IFs belong to one of the three major classes of cytoskeletal filaments, and they are important for maintaining mechanical integration. There are many kinds of IF proteins, and their expression is tissue-specific. Among them, vimentin is a major component of IFs in cells of mesenchymal origin. Even though the exact roles of vimentin are not determined yet, the analyses of the null mutant mice have revealed several defective phenotypes as follows: deficiencies in the modulation of vascular tuning (40), deficiencies in the mechanotransduction of shear stress (41), a cerebellar defect and impaired motor coordination (42), and impaired migration of fibroblasts into the wound sites (43). These results show that vimentin is necessary for maintaining mechanical flexibility of a cell.

Immunostaining demonstrated that the localization pattern of MICAL overlaps significantly with vimentin filaments in HeLa and 293 cells. Therefore, it is strongly suggested that MICAL is associated with vimentin filaments and that MICAL is one of the vimentin filament-associated proteins. There are many IF-associated proteins. Among them are plectin (44), fimbrin (45), calponin (46), MAP-2 (47), and bullous pemphigoid antigen-1 (BPAG-1) (48). These molecules have a binding capacity to IFs and are supposed to be important for maintaining cytoskeletal integrity. MICAL is also expected to be a member of these "IF-associated cytoskeletal integrators."

MICAL associates with CasL and vimentin. CasL is a downstream mediator of integrin-mediated signals and is important for cytoskeletal regulation. Although the exact biological functions of MICAL remain to be determined, the results suggest that MICAL could be a regulatory mediator that may transduce signals for IF regulation. Until now, several reports (49–51) have been made concerning the relationship between the integrin-mediated signal transduction and the regulation of IFs. Wu *et al.* (49) reported that integrin-associated protein (IAP/CD47) and proteins linking IAP with cytoskeleton medi-

ate signals between integrins and vimentin IFs. Modulation of these molecules influences the distribution pattern of vimentin and cell spreading. Plectin is also known as a linker molecule bridging integrins and IFs and is essential for hemidesmosome integrity and stabilization (50). Moreover, Sin *et al.* (51) suggested that vimentin IFs may be the reservoir of RhoA-binding kinase α (ROKα), which is a putative effector of RhoA, and may be regulated by integrin-mediated signals. Because our immunofluorescence study did not identify MICAL at the cell periphery, it may be difficult to expect the close biological interactions between MICAL and integrins. However, it is possible that MICAL may mediate further downstream signals via CasL.

We showed that MICAL associates with vimentin through the COOH-terminal region. Biological functions of other motifs, the CH domain and the LIM domain, remain to be elucidated. The CH domain was originally identified as a conserved motif in the calponin family proteins, and this motif is also present in a variety of other molecules, *e.g.* Vav and IQGAP-1 or -2. (52). Although our consensus for its biological function has not been completely settled, this domain is thought to be important as an actin-binding or IF-binding motif (45, 46, 52, 53), and it is suggested that a single CH domain may work as the interaction site with vimentin or other IF proteins. However, as for MICAL, the interpretation for this hypothesis is somewhat dazzling. We have found that bacterially expressed GST-MICAL CH domain fusion proteins can effectively make complexes with vimentin molecules *in vitro* (data not shown), whereas in the immunoprecipitation assay, we found that this region is not necessary for their interaction. Although we do not know the exact reason, their interaction may be interfered with by the structural conformation of other regions.

MICAL has one LIM domain in its central region. The LIM domain is a member of the Zn^{2+} finger motifs, and it is specified by its cysteine richness. LIM domains are found in many cytoplasmic and nuclear proteins, and they are supposed to be important for protein-protein interactions. Among the cytoplasmic LIM-containing proteins, many cytoskeletal regulatory molecules such as Paxillin, Zyxin, or Enigma are known, and it is anticipated that some biological functions of these molecules are mediated through LIM domains. Because MICAL is expected to be a possible cytoskeletal player, further investigation on this domain may reveal novel insights on this molecule.

In this study, we identified a novel molecule, MICAL, which may connect CasL and vimentin IFs. Until now, other related molecules, KIAA0750 (MICAL-2) and KIAA1364, have been identified from the human brain. Because these molecules show significant homology, we may call them "MICAL family proteins." At present, we know little about these molecules, and we are making further studies to clarify their functions. Finding more about the MICAL family proteins must provide important insights into the cellular biology.

Acknowledgment—We thank Dr. Masaki Inagaki (Aichi Cancer Center Research Institute, Japan) for kindly providing us with murine vimentin cDNA.

REFERENCES

1. Nojima, Y., Rothstein, D. M., Sugita, K., Schlossman, S. F., and Morimoto, C. (1992) *J. Exp. Med.* **175,** 1045–1053
2. Minegishi, M., Tachibana, K., Sato, T., Iwata, S., Nojima, Y., and Morimoto, C. (1996) *J. Exp. Med.* **184,** 1365–1375
3. Law, S. F., Estojak, J., Wang, B., Mysliwiec, T., Kruh, G., and Golemis, E. A. (1996) *Mol. Cell. Biol.* **16,** 3327–3337
4. Sakai, R., Iwamatsu, A., Hirano, N., Ogawa, S., Tanaka, T., Mano, H., Yazaki, Y., and Hirai, H. (1994) *EMBO J.* **13,** 3748–3756
5. Ishino, M., Ohba, T., Sasaki, H., and Sasaki, T. (1995) *Oncogene* **11,** 2331–2338
6. Alexandropoulos, K., and Baltimore, D. (1996) *Genes Dev.* **10,** 1341–1355
7. Petch, L. A., Bockholt, S. M., Bouton, A., Parsons, J. T., and Burridge, K. (1995) *J. Cell Sci.* **108,** 1371–1379
8. Nakamoto, T., Sakai, R., Honda, H., Ogawa, S., Ueno, H., Suzuki, T., Aizawa, S., Yazaki, Y., and Hirai, H. (1997) *Mol. Cell. Biol.* **17,** 3884–3897
9. Polte, T. R., and Hanks, S. K. (1995) *Proc. Natl. Acad. Sci. U. S. A.* **92,** 10678–10682
10. Burridge, K., Fath, K., Kelly, T., Nuckolls, G., and Turner, C. (1988) *Annu. Rev. Cell Biol.* **4,** 487–525
11. Clark, E. A., and Brugge, J. S. (1995) *Science* **268,** 233–239
12. Honda, H., Oda, H., Nakamoto, T., Honda, Z., Sakai, R., Suzuki, T., Saito, T., Nakamura, K., Nakao, K., Ishikawa, T., Katsuki, M., Yazaki, Y., and Hirai, H. (1998) *Nat. Genet.* **19,** 361–365
13. Steinert, P. M., and Roop, D. R. (1988) *Annu. Rev. Biochem.* **57,** 593–625
14. Robson, R. M. (1989) *Curr. Opin. Cell Biol.* **1,** 36–43
15. Fuchs, E., and Weber, K. (1994) *Annu. Rev. Biochem.* **63,** 345–382
16. Fuchs, E., and Cleveland, D. W. (1998) *Science* **279,** 514–519
17. Galou, M., Gao, J., Humbert, J., Mericskay, M., Li, Z., Paulin, D., and Vicart, P. (1997) *Biol. Cell* **89,** 85–97
18. Sattler, M., Salgia, R., Shrikhande, G., Verma, S., Uemura, N., Law, S. F., Golemis, E. A., and Griffin, J. D. (1997) *J. Biol. Chem.* **272,** 14320–14326
19. Ohashi, Y., Iwata, S., Kamiguchi, K., and Morimoto, C. (1999) *J. Immunol.* **163,** 3727–3734
20. Tachibana, K., Urano, T., Fujita, H., Ohashi, Y., Kamiguchi, K., Iwata, S., Hirai, H., and Morimoto, C. (1997) *J. Biol. Chem.* **272,** 29083–29090
21. Manie, S. N., Beck, A. R., Astier, A., Law, S. F., Canty, T., Hirai, H., Druker, B. J., Avraham, H., Haghayeghi, N., Sattler, M., Salgia, R., Griffin, J. D., Golemis, E. A., and Freedman, A. S. (1997) *J. Biol. Chem.* **272,** 4230–4236
22. Astier, A., Manie, S. N., Avraham, H., Hirai, H., Law, S. F., Zhang, Y., Golemis, E. A., Fu, Y., Druker, B. J., Haghayeghi, N., Freedman, A. S., and Avraham, S. (1997) *J. Biol. Chem.* **272,** 19719–19724
23. Liu, F., Hill, D. E., and Chernoff, J. (1996) *J. Biol. Chem.* **271,** 31290–31295
24. Garton, A. J., Burnham, M. R., Bouton, A. H., and Tonks, N. K. (1997) *Oncogene* **15,** 877–885
25. Kirsch, K. H., Georgescu, M. M., and Hanafusa, H. (1998) *J. Biol. Chem.* **273,** 25673–25679
26. Nakamoto, T., Yamagata, T., Sakai, R., Ogawa, S., Honda, H., Ueno, H., Hirano, N., Yazaki, Y., and Hirai, H. (2000) *Mol. Cell. Biol.* **20,** 1649–1658
27. Niwa, H., Yamamura, K., and Miyazaki, J. (1991) *Gene (Amst.)* **108,** 193–199
28. Ueno, H., Hirano, N., Kozutsumi, H., Sasaki, K., Tanaka, T., Yazaki, Y., and Hirai, H. (1995) *J. Biol. Chem.* **270,** 20135–20142
29. Nakamoto, T., Sakai, R., Ozawa, K., Yazaki, Y., and Hirai, H. (1996) *J. Biol. Chem.* **271,** 8959–8965
30. Kozak, M. (1986) *Cell* **44,** 283–292
31. Nagase, T., Ishikawa, K., Suyama, M., Kikuno, R., Miyajima, N., Tanaka, A., Kotani, H., Nomura, N., and Ohara, O. (1998) *DNA Res.* **5,** 277–286
32. Ren, R., Mayer, B. J., Cicchetti, P., and Baltimore, D. (1993) *Science* **259,** 1157–1161
33. Yu, H., Chen, J. K., Feng, S., Dalgarno, D. C., Brauer, A. W., and Schreiber, S. L. (1994) *Cell* **76,** 933–945
34. Sparks, A. B., Rider, J. E., Hoffman, N. G., Fowlkes, D. M., Quillam, L. A., and Kay, B. K. (1996) *Proc. Natl. Acad. Sci. U. S. A.* **93,** 1540–1544
35. Kamiguchi, K., Tachibana, K., Iwata, S., Ohashi, Y., and Morimoto, C. (1999) *J. Immunol.* **163,** 563–568
36. Knudsen, B. S., Feller, S. M., and Hanafusa, H. (1994) *J. Biol. Chem.* **269,** 32781–32787
37. Smit, L., van der Horst, G., and Borst, J. (1996) *J. Biol. Chem.* **271,** 8564–8569
38. Tanaka, S., Morishita, T., Hashimoto, Y., Hattori, S., Nakamura, S., Shibuya, M., Matuoka, K., Takenawa, T., Kurata, T., Nagashima, K., and Matsuda, M. (1994) *Proc. Natl. Acad. Sci. U. S. A.* **91,** 3443–3447
39. Kanda, H., Mimura, T., Morino, N., Hamasaki, K., Nakamoto, T., Hirai, H., Morimoto, C., Yazaki, Y., and Nojima, Y. (1997) *Eur. J. Immunol.* **27,** 2113–2117
40. Terzi, F., Henrion, D., Colucci-Guyon, E., Federici, P., Babinet, C., Levy, B. I., Briand, P., and Friedlander, G. (1997) *J. Clin. Invest.* **100,** 1520–1528
41. Henrion, D., Terzi, F., Matrougui, K., Duriez, M., Boulanger, C. M., Colucci-Guyon, E., Babinet, C., Briand, P., Friedlander, G., Poitevin, P., and Levy, B. I. (1997) *J. Clin. Invest.* **100,** 2909–2914
42. Colucci-Guyon, E., Gimenez, Y. R. M., Maurice, T., Babinet, C., and Privat, A. (1999) *Glia* **25,** 33–43
43. Eckes, B., Colucci-Guyon, E., Smola, H., Nodder, S., Babinet, C., Krieg, T., and Martin, P. (2000) *J. Cell Sci.* **113,** 2455–2462
44. Foisner, R., Traub, P., and Wiche, G. (1991) *Proc. Natl. Acad. Sci. U. S. A.* **88,** 3812–3816
45. Correia, I., Chu, D., Chou, Y. H., Goldman, R. D., and Matsudaira, P. (1999) *J. Cell Biol.* **146,** 831–842
46. Mabuchi, K., Li, B., Ip, W., and Tao, T. (1997) *J. Biol. Chem.* **272,** 22662–22666
47. Hirokawa, N., Hisanaga, S., and Shiomura, Y. (1988) *J. Neurosci.* **8,** 2769–2779
48. Yang, Y., Dowling, J., Yu, Q. C., Kouklis, P., Cleveland, D. W., and Fuchs, E. (1996) *Cell* **86,** 655–665
49. Wu, A. L., Wang, J., Zheleznyak, A., and Brown, E. J. (1999) *Mol. Cell* **4,** 619–625
50. Rezniczek, G. A., de Pereda, J. M., Reipert, S., and Wiche, G. (1998) *J. Cell Biol.* **141,** 209–225
51. Sin, W. C., Chen, X. Q., Leung, T., and Lim, L. (1998) *Mol. Cell. Biol.* **18,** 6325–6339
52. Castresana, J., and Saraste, M. (1995) *FEBS Lett.* **374,** 149–151
53. Gimona, M., and Mital, R. (1998) *J. Cell Sci.* **111,** 1813–1821

ELSEVIER

Immunology Letters 81 (2002) 59–64

Immunology Letters

www.elsevier.com/locate/

Expression of Notch ligands, Jagged1, 2 and Delta1 in antigen presenting cells in mice

Etsuko Yamaguchi, Shigeru Chiba, Keiki Kumano, Atsushi Kunisato, Tokiharu Takahashi, Tsuyoshi Takahashi, Hisamaru Hirai *

Department of Hematology and Oncology, Graduate School of Medicine, University of Tokyo Hospital, 7-3-1 Hongo, Bunkyo-ku, Tokyo 113-8655, Japan

Received 21 August 2001; accepted 31 October 2001

Abstract

Notch1 is indispensable for T cell development. It is anticipated that Notch1 and other Notch receptors expressed on the surface of thymic T cell precursors are activated by ligands present on environmental cells, including antigen presenting cells (APCs), and involved in positive and negative selections. Notch receptors on peripheral T cells may also be activated by ligands on APCs. Here, we examined the expression pattern of three Notch ligands, Jagged1, 2 and Delta1 in APCs by an immunofluorescence cell staining method and a reverse transcriptase-polymerase chain reaction (RT-PCR) method. Peritoneal macrophages were strongly positive for Jagged1 staining. In contrast, macrophages separated from spleen and dendritic cells (DCs) separated from spleen and thymus showed positive staining for all the three ligands at a similar intensity. An analysis by RT-PCR revealed that peritoneal and splenic macrophages and splenic and thymic DCs, show a distinct pattern in Notch ligand expression. These findings may represent that expression of various Notch ligands in APCs has a physiological relevance in each organ.

Keywords: Notch; Notch ligand; Jagged1; Jagged2; Delta1; Antigen presenting cells (APCs); Dendritic cells (DCs); Macrophage

1. Introduction

Notch proteins constitute a family of highly conserved transmembrane receptors that regulate cell fate decision during the development of many cell lineages in both vertebrates and invertebrates [1]. The Notch receptors and their ligands are highly expressed in the thymus and have been implicated in the early T cell development. It has also been reported that Notch1 gene is also expressed in the thymocytes and mature T cells [2–4]. Ligands for the Notch receptors must be expressed on the surface of cells physically associating with the target cells [5], since these ligands are present on the cell surface in the physiological conditions. It is, thus, expected that stromal cells in the thymus, spleen and other lymphoid tissues as well as thymic epithelial cells are candidates for Notch ligand-expressing cells that are required for precursor and mature T cells, Notch receptors on which are activated. We raised a question whether antigen presenting cells (APCs) such as macrophages and dendritic cells (DCs) in the lymphoid tissue function as a Notch-signal donor, in addition to the antigen presentation. Here we studied in detail the expression pattern of Notch ligands; Jagged1, Jagged2 and Delta1, in mouse APCs by immunofluorescence cell staining and reverse transcriptase polymerase-chain reaction (RT-PCR).

2. Material and method

2.1. Animals and cell preparations

C57BL/6 mice were purchased from Nippon Clea (Tokyo, Japan). In all experiments, 5–6-week-old female mice were used.

* Corresponding author. Tel.: +81-3-5800-6421; fax: +81-3-5689-7286.

E-mail address: hhirai-tky@umin.ac.jp (H. Hirai).

0165-2478/02/$ - see front matter
PII: S0165-2478(01)00326-1

2.2. Isolation of DCs from thymus and spleen

DCs were prepared from the thymus and spleen following an isolation protocol [6–8] with a modification, using six mice for each preparation. Briefly, the thymi and spleens were cut into small fragments and digested with collagenase type III (0.5 mg/ml; Worthington Biochemical Corporation) and DNase I (40 μg/ml, Wako Pure Chemical Industries, Ltd.) in RPMI 1640 medium supplemented with fetal calf serum (FCS) for 15–20 min at 37 °C with continuous agitation. The digested fragments were mixed by pipetting and filtered through a stainless-steel sieve with nylon mesh, and the cell suspensions were washed twice in phosphate-buffered saline (PBS) supplemented with 5% FCS and 5 mM EDTA (PBS–EDTA–FCS) containing 5 μg/ml DNase I. The cells were then resuspended in ice-cold iso-osmotic Optiprep solution (pH 7.2, density 1.061 g/cm^3, Nyegaard Diagnostics), containing 5 mM EDTA to dissociate DC-thymocyte complexes, and centrifuged at 3000 rpm for 30 min. A low-density fraction was suspended in PBS–EDTA–FCS after wash in the same buffer. The cells were resuspended in MACS buffer (Miltenyi Biotech) at 1×10^8 cells per ml and incubated with the MACS microbeads coated with an anti mouse CD11c antibody after blocking with an anti mouse IgG2b antibody. The cells were then passed over a MACS column and the cells retained in the column after washing were collected [2]. Separated cell populations were analyzed for purity by FACS and used as DC fractions. Splenic macrophages were obtained as an adherent cell population after the density gradient preparation using Lymphoprep solution (Nycomed) and overnight incubation at 37 °C in 5% CO_2. Peritoneal macrophages were obtained by washing the peritoneal cavity with cold PBS.

2.3. Flowcytometry

The DC fractions were stained with an FITC-conjugated anti I-Ab (Pharmingen), anti-CD8a (clone53.67, Pharmingen), anti-F4/80 (Dainihon Seiyaku) antibodies and a phycoerythrin(PE)-conjugated anti-CD11c antibody (clone N418, hamster IgG, Pharmingen). Ice-cold PBS was used for all the steps. Cell-surface antigens were analyzed using the CELLQEST program (Becton Dickinson Immunocytomety Systems) with the FACS Calibur flow cytometer (Becton Dickinson Immunocytomety Systems).

2.4. Immunofluorescence cell staining

The DC fractions from spleen and thymus as well as splenic and peritoneal macrophages were incubated for 1.5 h and overnight, respectively, in the chamber slide coated with FCS and human fibronectin (Wako Pure Chemical Industries) to have the DCs and macrophages adhere to the slides. After incubation, non-adherent thymocytes and lymphocytes were removed by washing with PBS. The slide-attached DCs and macrophages were fixed with −20 °C methanol for 10–15 min, air-dried, permialized with PBS containing 0.1% NP-40 for 10 min and incubated for 40 min with 5% BSA in PBS for blocking. The cell layer was then covered with goat antibodies against mouse Jagged1, Jagged2 and Delta1 (Santa Cruz Biotechnology), and a rat antibody against mouse F4/80 antibody (hybridomas were purchased from American Type Culture Collection (ATCC)), respectively, and incubated for 60 min. The washed cell layer was incubated with a fluorescein-conjugated anti goat IgG (ICN Pharmaceuticals) or Cy-3-conjugated anti-rat IgG (Jackson Immuno Research Labolatories) secondary antibodies for 45 min. After the wash with PBS, chamber-detached slides were mounted by cover slips with 50% glycerol in PBS with 2.5% 1,4-diazabicyclo[2,2,2]octane (Dabco, Sigma).

2.5. RT-PCR

The forward and reverse primers used for PCR were as follows: Delta1, CTGAGGTGTAAGATGGAAGCG and CAACTGTCCATAGTGCAATGG; Jagged1, TGCAGCTGTCAATCACTTCG and CAGAATGACGCTTCCTGTCG [9]; Jagged2, GTCCTTCCCACATGGGAGTT and GTTTCCACCTTGACCTCGGT [4]; mouse glyceraldehyde-3-phosphate dehydrogenase (G3PDH), GCATTGTGGAAGGGCTCATG and TTGCTGTTGAAGTCGCAGGAG.

Total RNA was isolated from cells using ISOGEN (Nippon gene) as manufacturer's instructions. After the treatment with DNAse I (GibcoBRL), random hexamer-primed cDNA was prepared from 500 ng of total RNA, using Superscript II (GibcoBRL) in a total volume of 20 μl. Semi-quantitative RT-PCR was performed as described previously [10]. Briefly, to standardize the template cDNA, a series of dilution was subjected to 25 cycles of PCR using a primer pair specific for G3PDH. After determining the relative cDNA concentration, specific primer pairs for Jagged1, Jagged2 and Delta1 were used to perform PCR to analyze the expression level of mRNA with the GeneAmp 9700 thermal cycler (Perkin–Elmer). The number of PCR cycle was determined for each primer pair between 25 and 35 cycles, to make the PCR yield depend on the amount of template cDNA. PCR products were analyzed by agarose gel electrophoresis followed by ethidium bromide staining.

3. Result

3.1. Characterization of cell fractions isolated from spleen and thymus

It is established that the mouse DCs are positive for MHC class II and CD11c [6,7,11]. Inversely, a majority of MHC class II+/CD11c+ cells are thought to be DCs in mouse. We, therefore, defined here these double positive cells as DCs. When the density and microbeads-purified cell fractions were analyzed by FACS, over 90 and 50% of the cells were positive for MHC class II and CD11c in the spleen- and thymus-derived fractions, respectively, in the three independent experiments. The majority of the MHC class II single positive cells were thought to be macrophages contaminating at less than 10% in the spleen-derived fraction (Fig. 1A) and about 20% in the thymus-derived fraction (Fig. 1B). In the thymus-derived fraction, double negative cells, majority of which were thought to be thymocytes, were contaminated at less than 3%.

3.2. Identification of Notch ligands on APCs by immunofluorescence cell staining

We next investigated whether the Notch ligand is expressed on the cell surface of peritoneal and splenic macrophages, and splenic and thymic DCs. In the peritoneal macrophage fraction, purity was virtually 100% in view of the positive staining with the F4/80 antibody (data not shown). These cells were positively stained with antibodies against Jagged1, Jagged2 and Delta1 (Fig. 2B–D), with the anti-Jagged1 antibody among them giving the strongest staining. The splenic macrophages were also positive for staining with all the three antibodies against the ligands. However, dominant staining with the anti-Jagged1 antibody was not observed and the intensity of staining was similar with all the three antibodies (Fig. 2F–H). Staining of the cells in the splenic and thymic DC fractions were technically difficult, because, the contaminating macrophages, rather than DCs, were apt to remain on the slide. Indeed, as much as 10–30% (Fig. 2J–L) and 30–50% of the remaining cells (data not shown) on the slide were macrophages, when prepared from the splenic and thymic DC fractions, respectively. Nevertheless, we were able to confirm that both splenic and thymic DCs were positive for staining with all the three anti-ligand antibodies, when double staining of the mixture of DCs and macrophages prepared from the splenic (Fig. 2J–L) and thymic (data not shown) DC fractions were performed using the anti F4/80 and respective anti-ligand antibodies.

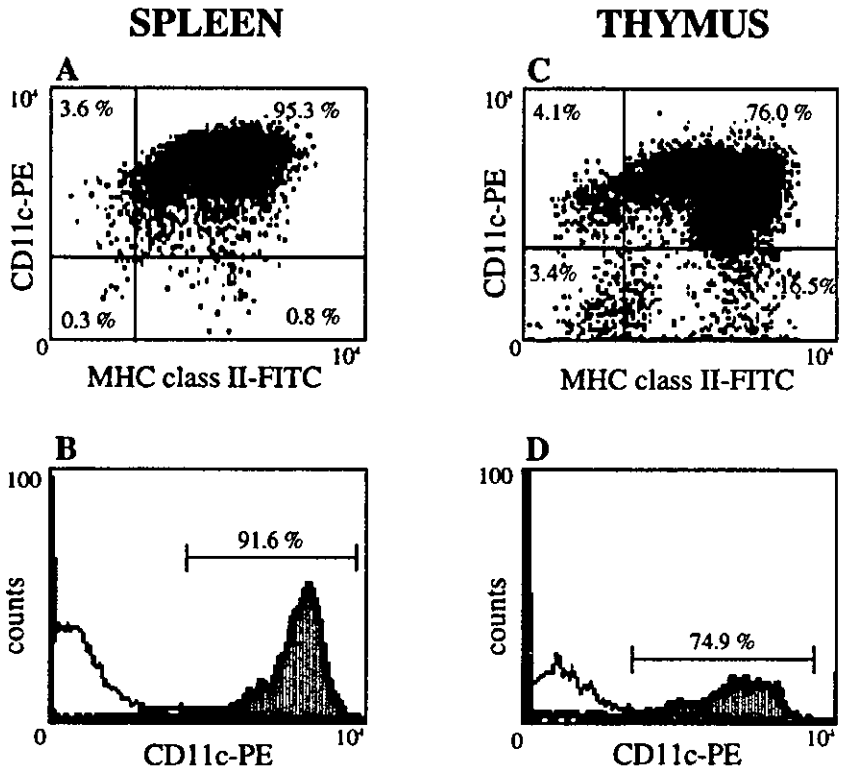

Fig. 1. FACS analysis for the splenic and thymic DC fractions. Cells separated from C57BL/6 mice were double-stained with a PE-conjugated anti-CD11c and FITC-conjugated anti-MHC class II antibody. Viable lymphocytes are shown after gating on forward and side scatters. Double positive cells were defined as DCs. Contaminated cells in the MHC class II-single positive cells are likely to be macrophages.

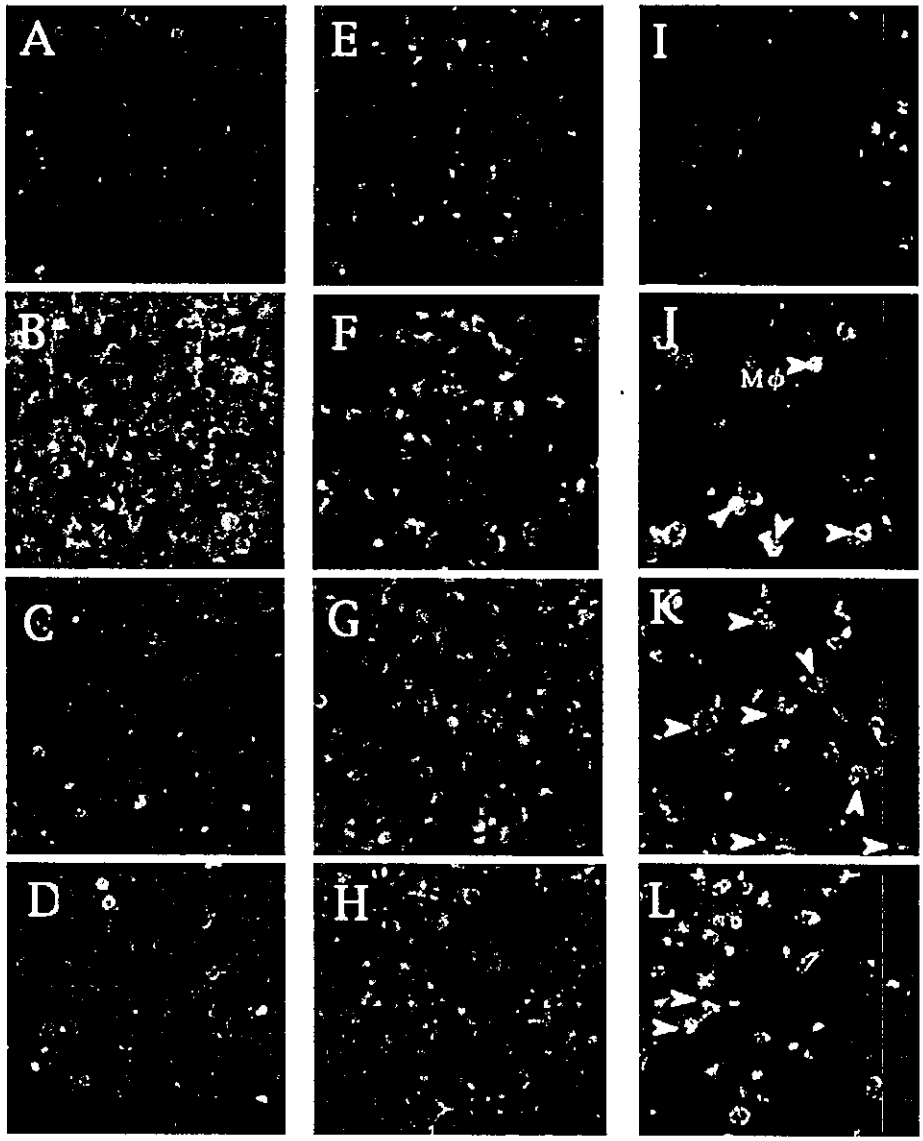

Fig. 2. Expression of Notch ligands in peritoneal macrophages, splenic macrophages and splenic DCs. Peritoneal macrophages (A–D), the cells were stained with a goat anti-Jagged1, -Jagged2 and -Delta1 antibody after overnight incubation on a plastic culture slide coated with human fibronectin and FCS (B–D). For negative control, goat IgG was used instead of the primary antibody (A). Splenic macrophages (E–H), The cells were stained with a rat anti-F4/80 antibody, plus one of the goat antibodies against Jagged1 (F), Jagged2 (G) and Delta1 (H) after incubation on a plastic culture slide coated with human fibronectin and FCS. Secondary antibodies used were a Cy-3 conjugated anti-rat IgG and FITC-conjugated anti-goat IgG antibody. For a control, goat IgG was used instead of the primary antibodies (E). All the cells were stained with an F4/80 antibody following the Cy-3 conjugated anti-rat IgG staining against control (data not shown). Splenic DCs (I–L), The cells were stained with a rat anti-F4/80 antibody, plus one of the goat antibodies against Jagged1 (J), Jagged2 (K) and Delta1 (L) after incubation on a plastic culture slide coated with human fibronectin and FCS. The secondary antibody used was Cy-3 conjugated anti-rat IgG and FITC-conjugated anti-goat IgG. For a control, goat IgG were used instead of the primary antibodies (I). Arrows indicate cells double-positive for F4/80 and a respective antibody against the ligands.

3.3. Expression analysis by RT-PCR

The peritoneal and splenic macrophages, and the cells in the splenic and thymic DC factions were analyzed for respective Notch ligand expression by RT-PCR. Difference in the expression pattern in the peritoneal and splenic macrophages, which was observed in the immunofluorescence staining, was reproduced by an RT-PCR analysis (Fig. 3). Expression pattern in either of these macrophage fractions was further different from that in the splenic or thymic DC fractions.

4. Discussions

There have been lines of evidence that indicate the role of Notch signaling in the T cell development [1,12–14]. There are also a few reports suggesting that Notch signaling play a role in mature T cells for their

antigen- or mitogen-induced activation [2,15]. However, the information about ligands that must trigger Notch signaling is limited. APCs are among the most likely candidates for the cells that physiologically give the Notch signaling to the developing and mature T cells [5,13].

There have been reports showing that by an RT-PCR and Northern blotting methods, Delta1 or Jagged1 is detected in macrophages, monocytes and splenic DCs [2,16]. It has also been reported that Jagged1 and Jagged2 are demonstrated in the thymus when an in situ hybridization technique is used [4]. However, no clear immunostaining has been shown for any Notch ligand, particularly for the fractionated or purified cell sources. We studied expression of the three Notch ligands which are thought to be expressed in the immune compartment, by the immunofluorescence- and RT-PCR-based methods, using fractionated and characterized cell sources. Purities of the peritoneal and splenic macrophages (positive for the anti-F4/80 antibody) and the splenic and thymic DCs (positive for anti CD11c and MHC class II antibody) were as high as 100, 100, >90 and about 70%, respectively. Using such highly purified cell preparations, we could understand that representative APCs express all the three Notch ligands examined, although we failed to detect the expression of Delta4, a newly identified mammalian Notch ligand [17] (data not shown). These results indicate that Jagged1, Jagged2 and Delta1, but not Delta4, function as a ligand for the Notch signaling in the precursor and mature T cells.

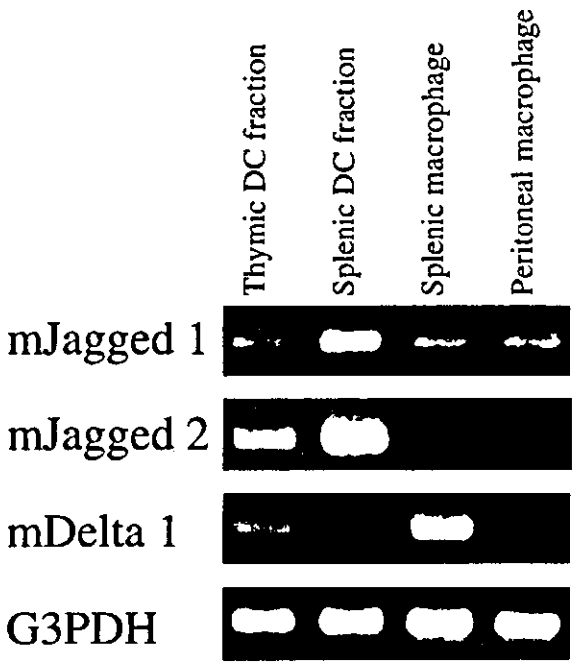

Fig. 3. Expression analysis of Jagged1, Jagged2 and Delta in peritoneal and splenic macrophage and splenic and thymic DC fractions by RT-PCR. Total RNA was extracted from each cell fraction. After cDNA was prepared from 500 ng of total RNA, a series of dilution was subjected to 25 cycles of PCR using a primer pair specific for G3PDH to standardize the template cDNA. After determining the relative cDNA concentration, specific primer pairs for Jagged1, Jagged2 and Delta1 were used to perform PCR for the analysis of expression level of mRNA. PCR products were analyzed by agarose gel electrophoresis followed by ethidium bromide staining.

Interestingly, macrophages prepared from two different sources, the peritoneal cavity and spleen, displayed distinct patterns of Notch ligand expression. Naturally, the environment for the macrophages in these tissues should be distinct from each other with regard to the variety of cytokines and concentration of each cytokine, variety of cells with which the macrophages make a contact. Recently, it was reported that the stimulation of macrophages with macrophage colony-stimulating factor, granulocyte-macrophage colony-stimulating factor and interleukin 3 resulted in upregulation of the Jagged1 expression [18,19]. Given these facts, a different expression pattern in the Notch ligands within the macrophage compartment is rational rather than unexpected. Similarly, it is reasonable that the DC fractions prepared from different organs showed distinct expression patterns from each other. These findings do not directly indicate the physiological roles of Notch ligands in APCs, but may suggest that the respective APCs constitute a part of the cells functioning as a signal donor for the precursor and mature T cells.

In the thymus, thymic epithelial cells may also be candidates for the Notch signal donor. Since DCs localize at more medullar region of the thymus, they may function at the later stages during the T cell development, while the thymic epithelium in the earlier stages. In both thymus and peripheral lymphoid tissues including spleen, stromal cells other than APCs may express Notch ligands and trigger Notch signaling. Furthermore, there is a suggestion that some T cells may express Notch ligands and function autonomously [4,5,15]. For the future understanding of Notch signaling in the entire signaling network in the precursor and mature T cells compartments, experiments performing downregulation and upregulation in each candidate for a Notch signal donor may give answers.

References

[1] M.L. Deftos, M.J. Bevan, Curr. Opin. Immunol. 12 (2000) 166–172.
[2] G.F. Hoyne, I.L. Roux, M. Corsin-Jimenez, K. Tan, J. Dunne, L.M.G. Forsyth, M.J. Dallman, M.J. Owen, D. Ish-Horowicz, J.R. Lamb, Int. Immunol. 12 (2000) 177–185.
[3] M.L. Deftos, Y.W. He, E.W. Ojala, M.J. Bevan, Immunity 9 (2000) 777–786.
[4] M.P. Felli, M. Marella, T.A. Mitsiadis, A.F. Campese, D. Bellavia, A. Vacca, R.S. Mann, L. Frati, U. Lendahl, A. Gulino, I. Screpanti, Int. J. Immunol. 11 (1999) 1017–1025.

[5] G.F. Hoyne, M.J. Dallman, J.R. Lamb, Immunology 100 (2000) 281–288.
[6] I. Ferrero, F. Anjuere, H.R. MacDonald, C. Ardavin, Blood 90 (1997) 1943–1951.
[7] F. Anjuere, P. Martin, I. Ferrero, M.L. Fraga, G.M. del Hoyo, N. Wright, C. Ardavin, Blood 93 (1999) 590–598.
[8] F. Radtke, I. Ferrero, A. Wilson, R. Lees, M. Aguet, H.R. MacDonald, J. Exp. Med. 191 (2000) 1085–1093.
[9] P. Jones, G. May, L. Healy, J. Brown, G. Hoyne, S. Delassus, T. Enver, Blood 5 (1998) 1505–1511.
[10] K. Kumano, S. Chiba, K. Shimizu, T. Yamagata, N. Hosoya, T. Saito, T. Takahashi, Y. Hamada, H. Hirai, Blood 98 (2001) 3283–3289.
[11] D. Vermac, M. Zorbas, R. Scollay, D.J. Saunders, C.F. Ardavin, L. Wu, K. Shortman, J. Exp. Med. 176 (1992) 47–58.
[12] J.P. Di Santo, F. Radtke, H.R. Rodewald, Curr. Opin. Immunol. 12 (2000) 159–165.
[13] B. Osborne, L. Miele, Immunity 11 (1999) 653–663.
[14] D.J. Izon, J.A. Punt, L. Xu, F.G. Karnell, D. Allman, P.S. Myung, N.J. Boerth, J.C. Pui, G.A. Koretzky, W.S. Pear, Immunity 14 (2001) 253–264.
[15] M.L. Deftos, E. Huang, E.W. Ojala, K.A. Forbush, M.J. Bevan, Immunity 13 (2000) 73–84.
[16] N. Singh, R.A. Phillips, N.N. Iscove, S.E. Egan, Exp. Hematol. 28 (2000) 527–534.
[17] T. Yoneya, T. Tahara, K. Nagao, Y. Yamada, T. Yamamoto, M. Osawa, S. Miyatani, M. Nishikawa, J. Biochem. 129 (2001) 27–34.
[18] K. Ohishi, B. Vamum-Finney, D. Flowers, C. Anasetti, D. Myerson, I.D. Bernstein, Blood 95 (2000) 2847–2854.
[19] K. Nomaguchi, S. Suzu, M. Yamada, H. Hayasawa, K. Motoyoshi, Exp. Hematol. 29 (2001) 850–855.

ACADEMIC PRESS

Biochemical and Biophysical Research Communications 294 (2002) 635–641

BBRC

www.academicpress.com

Analysis of gene expression profile in p130^{Cas}-deficient fibroblasts

Tetsuya Nakamoto,[a] Takahiro Suzuki,[a] Jinhong Huang,[b] Tomoko Matsumura,[a] Sachiko Seo,[a] Hiroaki Honda,[a,1] Ryuichi Sakai,[b] and Hisamaru Hirai[a,*]

[a] *Department of Hematology and Oncology, Graduate School of Medicine, University of Tokyo, 7-3-1 Hongo, Bunkyo-ku, Tokyo 113-8655, Japan*
[b] *Virology Division, National Cancer Center Research Institute, 5-1-1 Tsukiji, Chuo-ku, Tokyo 104-0045, Japan*

Received 10 May 2002

Abstract

p130^{Cas} (Cas) is a docking protein that becomes tyrosine phosphorylated in v-Src- or v-Crk-transformed cells and in integrin-stimulated cells. Cas −/− fibroblasts show defects in stress fiber formation, cell spreading, cell migration, and transformation by activated Src. To further characterize the role of Cas in signaling, we compared the expression profile in Cas −/− fibroblasts with that in Cas-re-expressing fibroblasts using the microarray methods. In Cas −/− fibroblasts, the expression of heme oxygenase 1 and caveolin-1 was reduced, but the expression of procollagen 1 α 1, procollagen 3 α 1, procollagen 11 α 1, elastin, periostin, TSC-36, and MARCKS was enhanced. The domains in Cas necessary for the change varied among these genes. Activated Src reduced the expression of most of these genes both in Cas −/− and in Cas +/+ fibroblasts. These results suggest the existence of signaling pathways that emanate from Cas to gene expression.

Keywords: p130^{Cas}; Microarray; Collagen; Elastin; Periostin; TSC-36; MARCKS; Caveolin; Heme oxygenase; Src

Extracellular matrix (ECM) is composed of collagens, fibronectin, vitronectin, elastin, laminins, and many other proteins. Cell-matrix interactions play a crucial role in a number of physiological and pathological processes including cell proliferation, migration, apoptosis, differentiation, metastasis, invasion, and wound healing. Focal adhesions are the site of cell-matrix attachment and integrins, cell surface receptors for ECM, are clustered to focal adhesions. Focal adhesions are composed of many other cytoskeletal and signaling proteins, such as FAK, Src, talin, paxillin, zyxin, tensin, and p130^{Cas} (Cas).

Cas was originally identified as a major tyrosine phosphorylated protein in v-Crk- or v-Src-transformed cells [1,2]. Cas contains an SH3 domain, the substrate domain that contains Crk SH2 binding motifs, the Src-binding domain, and the C-terminal domain that also binds to several proteins [2–5]. With these binding domains, Cas binds to many signaling molecules including FAK [6], PTP1B [7], PTP-PEST [8], C3G [9], CMS/CD2AP [10], CIZ [11], Nck [12], Chat [5], AND-34 [4], zyxin [13], and PI3K [14]. Cas is shown to be tyrosine phosphorylated in response to integrin stimulation [15,16] and transmits signals through several pathways, for example, through Crk-DOCK180 complex to Rac/JNK activation [17,18] and FAK/Cas/Crk complex is known to play a crucial role in cell migration [19,20].

Previously, we reported the phenotype of Cas-deficient mice [21]. Cas-deficient embryos died in utero at 11.5–12.5 days post-coitum showing marked congestion and growth retardation. Histological study of the embryo revealed disorganization of myofibrils and disruption of Z-disks in cardiocytes [21]. Furthermore, Cas-deficient fibroblasts showed impaired stress fiber formation, defects in cell migration, delayed cell spreading, and partial resistance to Src-induced transformation [21,22]. To further clarify the role of Cas in fibroblasts, we investigated the expression profile in Cas-deficient fibroblasts using microarray methods.

* Corresponding author. Fax: +81-3-5689-7286.
E-mail address: hhirai-tky@umin.ac.jp (H. Hirai).
[1] Present address: Department of Cancer Research, Research Institute of Radiation Biology and Medicine, Hiroshima University, 1-2-3, Kasumi, Minami-ku, Hiroshima-shi, Hiroshima 734-8553, Japan.

0006-291X/02/$ - see front matter
PII: S0006-291X(02)00527-2